4.0 SHORELINE FAULT ZONE

The purpose of this section is to provide a detailed description of the seismic characteristics of the Shoreline fault zone as developed from extensive geologic, geophysical, and seismological data bases and analyses summarized in the previous sections. This description includes data and results considered in the Progress Report (PG&E, 2010a) and developed subsequently. The current understanding of the Shoreline seismicity lineament is discussed in Section 4.2, and the geological and geophysical characteristics of the Shoreline fault zone are discussed in Section 4.3. Section 4.4 presents the current understanding of the recency of fault activity and maximum slip rate of the Shoreline fault zone, and Section 4.5 discusses the kinematic relationship between the Shoreline fault zone and the Hosgri and Southwestern Boundary fault zones.

4.1 Introduction

Following identification of the Shoreline seismicity lineament in 2008 (published in Hardebeck, 2010), an extensive program to acquire and interpret new geological, geophysical, and bathymetric data was performed in 2009 and 2010, as described in Section 2. Based on these studies, a coast-parallel, near-shore bedrock fault zone was identified that lies within the epicentral uncertainty of the seismicity lineament. Given the close spatial association of the fault zone to the seismicity lineament, PG&E interprets that this fault zone, called the Shoreline fault zone, is producing the observed seismicity.

Plate 1 shows the location of the Shoreline fault zone in relation to the observed seismicity and the interpreted onshore and offshore geology. The earthquake data are from Hardebeck (2010) and are used as a primary basis for analysis. The onshore and offshore geologic mapping is presented in more detail in Appendix B.

The Shoreline fault zone is divided into three segments based on differences in the geologic and geomorphic expression of surface and near-surface faulting, intersections with other mapped structures, features observed in the high-resolution magnetic field data, and variations in the continuity, trend, and depth of the seismicity along the lineament. The segments of the Shoreline fault zone are named the North, Central, and South segments (Figure 4-1a). Similarly, the Shoreline seismicity lineament is divided into three distinct, en echelon sublineaments, referred to as the Northern, Central, and Southern seismicity sublineaments (Plate 1, inset). The three Shoreline fault zone segments correspond spatially in both length and location to the three seismicity sublineaments, supporting the segmented nature of the fault zone. These fault zone segments are considered as possible rupture segments in the seismic source characterization discussed in Section 5 of this report.

There are two important differences between the discussion in the Progress Report (Figure 4-1b; PG&E, 2010a) and the present report. First, the current North segment was previously referred to as the "Northern Seismicity Lineament" because at that time the evidence of faults in the bedrock using the 2008 seismic reflection data had not been seen. Second, the current N40W fault was previously referred to as the Northern Segment and was included as an inactive segment of the Shoreline fault zone in the Progress Report. Although a submerged wave-cut platform estimated to be at least 75,000 year old does not appear to be vertically offset by the N40W fault, the fault's proximity to the Northern seismicity lineament and its similarity to the

South and Central segments of the Shoreline fault zone are the basis for considering it to be an alternative northern continuation of the Shoreline fault zone in the seismic source characterization (Section 5).

The following sections provide a discussion of the Shoreline seismicity lineament (Section 4.2) and a description of the characteristics of the Shoreline fault zone (Section 4.3). Table 4-1 summarizes these characteristics and compares them to the characteristics described in the Progress Report (PG&E, 2010a).

4.2 Shoreline Seismicity Lineament

The Progress Report (PG&E, 2010a) concluded that the Shoreline seismicity lineament (Figure 4-2a) is based on accurately located microearthquakes**.** This conclusion was based primarily on the tests of the relative relocations by Hardebeck (2010) by independent reviewers Dr. Clifford Thurber using the tomoDD program (Zhang and Thurber, 2003) (which Hardebeck also used) and Dr. Felix Waldhauser using hypoDD (Waldhauser and Ellsworth, 2000). The results of the tests by Drs. Thurber and Waldhauser are presented in Appendix C (C-1 and C-2). Thurber performed two tests using Hardebeck's phase data and waveforms. The first test used tomoDD and Hardebeck's 3-D velocity model (Hardebeck, 2010) to successfully replicate her relocations. The second test relocated the 49 earthquakes that comprise the Shoreline seismicity lineament using tomoDD and his preferred velocity model and input parameters. Waldhauser used Hardebeck's phase data and waveforms and tested the McLaren and Savage (2001) 1-D model and the Hardebeck 3-D model in hypoDD, and Hardebeck's 3-D model in a hybrid version of his program. The results from both reviewers also showed a lineament (Figure 4-2, parts a through c, and Appendix C), although Thurber's locations are generally shifted about 0.5 km farther offshore than Hardebeck's. The pattern of Waldhauser's locations is slightly more diffuse than the patterns that the Hardebeck and Thurber locations exhibit. These comparisons show that most of the 49 earthquakes as processed by the three researchers exhibit essentially the same evidence for the interpreted seismicity lineament.

Cross sections of the three sublineaments for Hardebeck, Thurber, and Waldhauser are shown on Figure 4-2, parts d through f. Thurber's locations are approximately 1 km shallower than the Hardebeck locations. The Waldhauser hypocenter depths are quite similar to Hardebeck's. These results were used to establish the ± 0.5 km epicentral and ± 1.3 km depth uncertainties of the earthquakes comprising the seismicity lineament (PG&E, 2010a). (See Section 4.2.2 below for additional details.)

The Hardebeck (2010) seismicity lineament parallels the coast and extends for a distance of approximately 23 km from an uncertain intersection with the Hosgri fault zone on the north to south of Point San Luis on the south (Plate 1 inset). The sublineaments are separated by en echelon offsets of approximately 0.5–1 km. The Southern sublineament is the least well defined and consists of eight earthquakes, although one of these earthquakes is the largest (M_L 3.5) in the entire lineament. The Southern sublineament trends slightly more westerly than the geologically defined South segment of the Shoreline fault zone (Figure 4-2a). In cross-section view, the hypocenters form a vertical alignment to a depth of about 8 km (Figure 4-2d). The Central sublineament is well defined, both in map and cross-section views and contains 16 earthquakes (Figure 4-2, parts a and d). It forms a vertical alignment to a depth of 8–10 km and closely

aligns with the geologically and geomorphologically well-defined Central segment of the Shoreline fault zone. The Northern sublineament contains up to 26 earthquakes and is defined by more diffuse and deeper seismicity (up to 13–15 km) compared to the Central sublineament and may reflect a complex intersection with the Hosgri fault zone, as discussed in Section 4.2.4. In map view, the Northern sublineament aligns with the North segment of the Shoreline fault zone, and trends more westerly than the adjacent N40W fault, an alternative but less preferred structural association for the Northern Shoreline seismicity sublineament, as discussed in Sections 4.2.4 and 4.3.

In the following sections, additional analyses and details of the Shoreline seismicity lineament are provided, including earthquake statistics and earthquake location uncertainties, analyses of epicentral and hypocentral patterns, and an analysis of the association of the Northern seismicity sublineament with the Hosgri fault zone. A description of pre-1988 historical earthquakes within the Shoreline fault zone study area is also provided.

4.2.1 Seismicity Lineament Data Statistics

A total of 49 earthquakes occurred between 1988 and 2008 within the seismicity lineament as defined by Hardebeck (2010). The magnitude range is 0.8 to 3.5 and the depth range is 2–15 km. The magnitude 3.5 earthquake occurred on 10 August 2000 at the southern end of the Southern seismicity sublineament. This earthquake is reported as a local magnitude (M_L) event, and the other earthquakes ($M \leq 2.9$) are reported as duration magnitudes (M_d). The M_L 3.5 event is classified as a small event, whereas the smaller earthquakes are classified as microearthquakes (Lee and Stewart, 1981).

Thurber's preferred data set contains 43 earthquakes (Appendix C). The 6 earthquakes not used by Thurber are either (1) earthquakes that relocated away from the lineament formed by most of the earthquakes or (2) earthquakes that were removed from the final data set because their computed locations were unstable. An example is the M_L 3.5 event, which was not included in Thurber's final run because its location was above the ground surface. In contrast, Hardebeck's relocation for this event was stable and converged at a depth of 3.7 km depth using her parameters in tomoDD.

The earthquakes that comprise the seismicity lineament have occurred fairly uniformly over time between 1987 and 2008 (Figure 4-3a) at an average rate of about 2.3 earthquakes per year. Figure 4-3b is a log-linear plot of the cumulative number of Shoreline lineament earthquakes versus magnitude. From this plot, the magnitude level of completeness is approximately 1.3. A *b*-value of 0.93 is estimated using the method of Weichert (1980). This value is consistent with the *b*-value of 0.91 from Reasenberg and Jones (1994) for their Southern California recurrence model.

4.2.2 Earthquake Location Uncertainties

There are three key factors considered in estimating earthquake location uncertainties for the offshore earthquakes of the Shoreline seismicity lineament, as discussed in the following two subsections. The three factors are the effect of limited azimuthal distribution of the on-land seismographic stations in the effort to triangulate the offshore earthquake locations, the level of accuracy of the velocity model, and the proximity of the closest stations to the epicenter. In the

third subsection, the method used to estimate the average location errors for the 49 earthquakes that comprise the lineament is explained.

Offshore Earthquake Locations

The accuracy of earthquake locations is directly related to seismographic station numbers and spacing. Figure 2-2 shows that the seismographic coverage in the central coast region has evolved and improved with time (McLaren and Savage, 2001). The main network design factors that contribute to robust earthquake locations are seismographic station spacing, azimuthal coverage, and accurate S-wave and P-wave arrival times. The closest station distance controls the depth accuracy, and azimuthal coverage controls the epicentral accuracy. The integrated PG&E−USGS station spacing is about 10–15 km within about 30 km from the coast. This station distribution translates to fairly good depth control for onshore earthquakes in the depth range of 5–10 km. Offshore earthquakes, such as those occurring along the Shoreline seismicity lineament 0–3 km offshore, have the inherent problem of lack of adequate station distribution, resulting in gaps of azimuthal coverage generally greater than 180 degrees and reduced depth control as the distance offshore increases. The five PG&E 3-component analog stations that have been in operation since 1987 have compensated somewhat for the lack of station distribution by improving the accuracy of picking S-wave arrivals. Since 2006, the PG&E station upgrades have improved data quality, but the basic geometry of monitoring the offshore has not changed.

Accuracy of the Velocity Model

An accurate velocity model is also important for accurate absolute locations of earthquakes. Traditionally, inverting arrival time data for catalog locations has been accomplished using a 1-D velocity model and applying it across a region with station corrections that compensate for path effects (e.g., *Hypoinverse*; Klein, 2002). Three-dimensional velocity modeling is used to account for lateral variations in structure, and relative arrival times from waveform cross-correlation and double-difference methods are used to image seismicity features more sharply, such as was done by Hardebeck (2010).

For Hardebeck's San Luis Obispo subregion, which includes the Shoreline and Hosgri fault zones, her velocity modeling results in a reduction in the root mean square (RMS) of the cross-correlation relative arrival times from 0.39 seconds from the 3-D starting model to 0.005 seconds for the final 3-D model. Hardebeck performed a validation of the model by relocating known blasts from a 1986 reflection/refraction program. The blasts occurred both onshore and offshore. The offshore blasts were located about 10 km north and south of the Shoreline seismicity lineament, in Estero Bay and San Luis Bay (Hardebeck, 2010, Fig. 5). The RMS shift from the true shot locations is 1.2 km horizontally and 1.3 km vertically, with the largest shift in the offshore shot locations. The location errors in the offshore blasts are an indication that as long as the earthquakes and blasts are occurring outside the network, there will be an inherent error or uncertainty in their locations.

Uncertainties from Comparing Earthquake Locations Using Different Location Methods

Earthquake location uncertainty is estimated using Hardebeck's, Thurber's, and Waldhauser's uncertainty estimates and the uncertainties based on the average horizontal and vertical shifts of the earthquake locations within the lineament that were obtained from the Hardebeck and Thurber relocations. Table 4-2a lists the absolute and relative uncertainty estimates for the three

results. Table 4-2b lists the average and median differences between the various location methods, 1-D, 3-D, and tomoDD.

Hardebeck (2010) estimated the absolute earthquake location uncertainty by relocating shots with known locations. For 13 shots located inside her 3-D velocity model, the RMS shift from the true location was 0.9 km horizontal and 1.3 km vertical. She concluded that the absolute uncertainty of the earthquake locations, which should be better located than the shots, was ≤ 0.9 km horizontal and ≤ 1.3 km vertical. She acknowledges that the offshore shot location errors are larger.

Hardebeck also estimated uncertainties for her San Luis Obispo region based on the stability of the locations determined using various location methods. The median absolute shift between her hypoDD and 3-D locations is 470 m horizontal and 450 m vertical. The median absolute location shift between her hypoDD and tomoDD locations is 390 m horizontal and 510 m vertical.

In a similar approach, the location results are compared between 1-D, 3-D, Waldhauser's hypoDD, and Thurber's preferred tomoDD locations specifically for the earthquakes that comprise the Shoreline seismicity lineament. The averages and standard deviations are described in Table 4-2b. The average and median shift values between the two tomoDD runs are similar. For this report, the more conservative average horizontal shift of 0.51 km and average vertical shift of 1.33 km were chosen for use in evaluating the significance of location uncertainties.

4.2.3 Relation of the Shoreline Seismicity Lineament to Earthquakes Prior to 1988

Earthquake records prior to the deployment of the PG&E seismic network in 1988 were searched to evaluate whether additional earthquakes have occurred on the Shoreline seismicity trend. The search can be broken down into two time intervals: earthquakes prior to 1970 and earthquakes between 1970 and 1987.

Earthquakes Prior to 1970

A search of the historical database prior to 1970 and prior to local seismic networks (NCEDC, 2010; McLaren and Savage, 2001) showed two M 5 earthquakes that occurred in 1913 and 1916 in the vicinity of the seismicity lineament in the past 100+ years. Considering the location uncertainty of 10–20 km (PG&E, 1988; McLaren and Savage, 2001) for these events, it is possible that they could have been associated with the South segment of the Shoreline fault zone or one of the faults in the Southwestern Boundary fault zone. The 10 km radius circles of uncertainty are shown on Figure 4-4 for the two events. These earthquakes are discussed in the following paragraphs.

- 20 October 1913: This earthquake was located by Toppozada (1987) in the offshore region near Pismo Beach and Arroyo Grande. It was strongly felt in Pismo Beach and Arroyo Grande and as far south as Santa Barbara and Carpenteria. McLaren and Savage (2001) noted that it could have occurred on a fault within the Southwestern Boundary fault zone. The published location is about 5 km southeast of the easternmost seismicity in the Shoreline seismicity lineament.

- 1 December 1916: This earthquake occurred north of the 1913 event. Bolt and Miller (1975) located it directly offshore of Avila Beach in San Luis Obispo Bay, although the published coordinates place it north of Avila Beach. Some of the Union Oil refinery smokestacks toppled over. Landslides were reported in the canyon behind Avila and in Dairy Canyon, 2 miles north of Avila, and the event was strongly felt in San Luis Obispo (McLaren and Savage, 2001). A local newspaper article also reported, "… an upheaval of the waters in the Bay of San Luis Obispo, as the trembling continued out to sea" (McLaren and Savage, 2001). Avila Beach is about 4 km northeast of the southern end of the Shoreline seismicity lineament.

Earthquakes from 1970 to 1987
The USGS catalog data from 1970 to 1987 shows 3–5 microearthquakes in the vicinity of the Shoreline fault zone (Figure 4-5a), allowing for possible large errors in their routine locations. Hardebeck relocated these earthquakes using hypoDD and the 3-D velocity model she developed using the post-1987 data (Hardebeck, 2010). Her results showed that only one of these microearthquakes is likely to have occurred within the Shoreline seismicity lineament (in the Southern sublineament) during this time period (Figure 4-5b).

4.2.4 Data Interpretation

This section discusses the relationship between the seismicity patterns and other features of the Shoreline seismicity lineament and the geologic structure of the Shoreline fault zone. The interpretation of the relationship between the Hosgri fault zone and the Shoreline fault zone is also discussed.

Comparison of Lineament Patterns
A comparison of Hardebeck's relocations to those of Thurber and Waldhauser (Figure 4-2) show that although the earthquake patterns between the results vary somewhat, they are consistent within the bounds of the ± 0.5 km epicentral location uncertainty and the ± 1.3 km vertical uncertainty estimated for the Hardebeck locations. Figures 4-2a-c show quite similar seismicity lineaments in map view among the three different relocation efforts, particularly along the Central and Southern sublineaments. The cross-section views (Figures 4-2d-f) show similar hypocentral patterns of scattered activity between about 2 and 10 km depth in the Southern and Central sublineaments, a fairly abrupt deepening of seismicity to 12–15 km at the south end of the Northern sublineament, and a diffuse zone of deep earthquakes along the Northern sublineament as it approaches the Hosgri fault zone. A general result of this comparison is that, while there are slight differences in the detailed patterns of each of the three maps and sets of vertical sections, such as variations in depth groupings and slight differences in the locations of offsets of epicenters along the mapped alignments, there are no compelling reasons not to accept all the relocations as defining (within the selected uncertainty bounds) a vertical surface that is deeper to the northwest and gently sinuous in map view.

As stated in the Progress Report (PG&E, 2010a), a pronounced seismicity lineament along the southern Irish Hills coast was not previously identified using 1-D catalog locations, as shown on Figure 4-6a. What was visible was a scattering of earthquake epicenters between the coastline and the Hosgri fault zone and staying within about 4 km of the coastline toward Point San Luis to the southeast. Previously, PG&E interpreted this diffuse pattern as due to scattered activity

along small faults that likely branched off the Hosgri fault zone (Plate 3, PG&E, 1988), and possible seismicity related to the Olson Hill deformation zone. On Figure 4-6b, Hardebeck's 3-D locations also show scattered events within the same broad swath as Figure 4-6a; Figure 4-6b also shows the narrow, linear feature now called the Shoreline seismicity lineament.

In general, the results of both 1-D and 3-D absolute location methods often yield seismicity maps that do not resolve seismicity lineaments and other features that can be associated with active geologic structures, especially in an offshore region and outside spatially restricted seismic networks (see Thurber's review, Appendix C). The sophisticated earthquake relocation techniques such as those developed and applied by Thurber, Waldhauser, and Hardebeck are intended to provide more highly resolved relationships between microearthquake and larger earthquakes and the geologic structure of active tectonic and volcanic regimes. For example, McLaren et al. (2008) used hypoDD to relocate the 22 December 2003 San Simeon earthquake and aftershocks. Their results were able to resolve the relationship of the main shock to the main fault plane and backthrust plane defined by the aftershocks.

Compared to the 1-D locations, most of the 3-D offshore epicenters, including the earthquakes on the Hosgri fault zone, shift about 0.5 km to the east (Figure 4-6a–b). This systematic change in a group of relocated earthquakes is a normal product of the application of advanced relocation technology, including better-calibrated 3-D seismic velocity models. While such relocations usually provide better resolution of possible geometric or structural features of the seismicity, the locations may still have systematic biases largely due to remaining errors in the velocity model used in the relocations. Therefore, it is important to use high-resolution geophysical and geological techniques to attempt to constrain the location and geometry of the geologic structure in the vicinity of the structures that have been resolved in the seismicity data. In particular, the absolute locations of geologic structures such as the Shoreline fault zone are determined by other investigations discussed in this report, not by the seismicity. The spatial features of the Shoreline seismicity lineament (including consideration of the hypocentral location uncertainties) that are inferred to reflect structural features at depth are evaluated with respect to the geometry and other characteristics of the independently determined surface and subsurface geologic structures. In combination, these data are used to assess the potential for the geologically defined Shoreline fault zone to be the structure that is releasing the observed seismicity and possibly larger future earthquakes.

Shoreline Seismicity Lineament Focal Mechanisms

The focal mechanisms shown on Figure 4-7 are from Hardebeck (2010) using the program HASH (Hardebeck and Shearer, 2002) and from the USGS catalog using the algorithm FPFIT (Reasenberg and Oppenheimer, 1985) that uses P-wave first-motion data from earthquakes located with a 1-D velocity model. HASH computes P-wave first-motion focal mechanisms using takeoff angles observed from ray tracing in the 3-D seismic velocity model. FPFIT is a grid-search algorithm that finds the best double-couple solution. The FPFIT mechanisms have been filtered to include only those earthquakes with unique, good-quality solutions that use 25 or more P-wave first motions and that have converged to the solution by finding the minimum misfit solution.

HASH assigns mechanism quality (A, B, C, and D) based on the solution stability with respect to the uncertainty in the take-off angles and polarity observations. Quality D mechanisms are from

those earthquakes that did not meet the criteria of Quality A to C earthquakes, but were considered adequate upon examination of the polarity data (at least 6 P-wave first motions) and the computed focal mechanisms (Hardebeck, 2010). Hardebeck (2010) also computed composite focal mechanisms for selected sets of earthquakes in the offshore and southern parts of the study area where there was limited azimuthal coverage. She grouped together earthquakes that were clustered in space (Figure 4-7).

Due to the stringent nature of the acceptance parameters, including robust azimuthal station distribution, Hardebeck's highest quality focal mechanisms (Qualities A to C) are all onshore (Figure 4-7). The offshore focal mechanisms thus include her Quality D and composite focal mechanisms and the FPFIT mechanisms from the USGS Northern California Earthquake Data Center catalog (http://www.ncedc.org/ncedc/catalog-search.html).

The offshore focal mechanisms on Figure 4-7 show predominantly strike-slip motion, particularly along the Hosgri fault zone and the Central sublineament of the Shoreline seismicity lineament. Scattered throughout are reverse and oblique-reverse focal mechanisms, and a few normal mechanisms. Focal mechanisms near the Northern sublineament are predominantly strike-slip and oblique-reverse. Mechanisms along the Central sublineament, including the composites, show consistent right-lateral, strike slip along northwest-trending fault planes, consistent with the orientation of the Central sublineament. Mechanisms along the Southern sublineament show normal and oblique-normal fault motion. The northeast-trending nodal planes of the pure normal mechanism at the south end of the Southern seismicity lineament, which is a Quality D focal mechanism, are not consistent with either the mapped orientation of the northwest-trending southern sublineament, or with Hardebeck's composite mechanism (Figure 4-7). The HASH mechanism for the M_L 3.5 event near the end of the Southern sublineament shows normal-oblique motion along a northwest-trending fault plane and is consistent with the mapped lineament orientation. The nearly pure strike-slip FPFIT mechanism for the M_L 3.5 event and Hardebeck's strike-slip composite mechanism for the small group of earthquakes near the M_L 3.5 event is evidence that the Southern sublineament is dominantly strike-slip, but with some normal-oblique fault motion.

Association of the Northern Seismicity Sublineament with the Hosgri Fault Zone
As described in the previous subsections of Section 4.2, the seismicity characteristics of the Southern and Central sublineaments have the following attributes:

- Earthquake epicenters are located along a nearly straight-line segment within the horizontal location uncertainty of 0.5 km.
- Earthquake hypocenters are distributed nearly vertically beneath the nearly straight line of the sublineament.
- The deepest earthquakes associated with either sublineament are no deeper than 10 km (8 km for the Southern sublineament).
- The predominant style of faulting as exhibited by focal mechanisms is right slip along a plane parallel to the strike of the lineament; however, there are outliers in each segment.

The pattern of the Northern seismicity sublineament, however, varies over its length. Beginning at its southeast end, the lineament exhibits the same characteristics as the Central and Southern

sublineaments, with the exception that the southeastern half of the Northern sublineament does not have any focal mechanism data.

However, as the projected Northern sublineament approaches the Hosgri fault zone, the following changed characteristics are observed:

- Earthquake epicenters diffuse outside of the collinear pattern defined by 0.5 km uncertainty (Plate 1 and Figure 4-8a), and it is not clear where the seismicity associated with the lineament ends and the seismicity associated with the Hosgri fault zone begins.
- Focal mechanisms include greater diversity than predominantly strike-slip (Figure 4-8a).
- Focal mechanisms at the western end have planes rotated closer to the strike of the Hosgri.
- The trend of the Northern sublineament is more northerly than the other two sublineaments, and appears to be bending northward.

This interaction is ultimately significant to interpreting the relationship between the Shoreline fault zone and the Hosgri fault zone, so it is extensively explored. To begin, the seismicity and focal mechanisms are projected onto cross sections perpendicular to the Hosgri fault zone and the Shoreline seismicity lineament, A-A′ and B-B′ on Figures 4-8a and 4-8b. The earthquakes that define the Northern seismicity sublineament are plotted in red in both cross sections for comparison. Also shown on cross section A-A′ are (1) the projection of an interpreted nearby common-depth point (CDP) seismic-reflection profile (Comap profile GSI-85; PG&E, 1988) showing the two steeply east-dipping branches of the Hosgri fault zone (cross section K-K′), and (2) linear projections of four possible average dip angles of the Hosgri fault zone ranging from 90 to 70 degrees to the northeast. Overall, the seismicity projected normal to the Hosgri fault zone (cross-section A-A′) fit reasonably well along an 80- to 85-degree east-dipping fault zone, especially when the red earthquakes of the Shoreline seismicity lineament are included below depths of 11 km. This pattern is consistent with the steeply east-dipping faults interpreted from the 1986-vintage CDP seismic reflection profile, and suggests that a viable alternative explanation for at least some of the earthquakes along the Northern seismicity sublineament is that they are part of the Hosgri fault zone, and not part of a separate Shoreline fault zone.

More detailed interpretations of the Hosgri fault zone at depth based on the seismicity data are ambiguous. For example, it is not clear whether the locations and focal mechanisms of the shallow earthquakes between about 3 and 8 km deep at the west side of cross section A-A′ are showing a vertically dipping west branch of the Hosgri fault zone or a steeply east-dipping west branch that connects with the central and east branches of the Hosgri fault zone below about 7 km depth. However, the strike-slip focal mechanisms of these shallow earthquakes are consistent with a vertically dipping west branch. Also, whereas the seismicity is not consistent with a Hosgri fault zone dipping approximately 70 degrees northeast or less to depth, the data cannot distinguish between a steeply (approximately 80 degrees) northeast-dipping Hosgri fault zone to depth and a northeast-dipping fault zone in the upper few kilometers (as interpreted from the CDP seismic reflection profile) that steepens to subvertical at depth.

In comparison to the diffuse seismicity projected normal to the Hosgri fault zone (cross section A-A′), the red earthquakes attributed to the Shoreline seismicity lineament plot in an aligned,

vertical pattern in cross section B-B′. The earthquakes between about 11 and 13 km that provide a reasonable fit to an 80- or 85-degree northeast-dipping Hosgri fault show a distinct vertical pattern on the Shoreline cross section B-B′. The earthquakes between about 4 and 9 km depth show an overall subvertical alignment, and in detail suggest a zigzag pattern that may indicate along-strike structural complexity. Also, focal mechanisms in this depth range show reverse and reverse-oblique fault motion along varying fault planes. As there are no earthquakes located shallower than about 4 km, the updip projection of the causative fault zone is unclear. Alternatives include (1) a buried fault that does not penetrate the upper few kilometers of crust; (2) an emergent, subvertical fault that coincides with the North segment of the Shoreline fault zone; and (3) an emergent fault that coincides with the more northerly striking N40W fault (Plate 1 and Section 4.3.1). Thus, whereas much of the seismicity along the Northern sublineament may record activity on the Hosgri fault zone, the overall pattern supports the preferred interpretation that the seismicity is associated with a distinct subvertical fault, the North segment of the Shoreline fault.

4.3 Geological and Geophysical Characterization of the Shoreline Fault Zone

Additional investigations completed since the Progress Report (PG&E, 2010a) have led to an improved understanding of the fault, including information on fault location, geometry, segmentation, slip rate, and relationship to the Hosgri fault zone, Southwestern Boundary fault zone, and older Tertiary structures.

The nomenclature used in this report for the Shoreline fault zone is presented in Table 4-1 and Figure 4-1. The characteristics of the Shoreline fault zone were developed from the following:

- Geologic and geomorphic interpretation of MBES bathymetric imagery (Appendix B).
- Assessment of submerged marine terraces from MBES bathymetric imagery and high-resolution seismic-reflection profiles (Appendix I).
- Correlation of geologic units and structures onshore and offshore (Appendix B) using a low-tide LiDAR base map (Appendix G).
- Reinterpretation of offshore diver and core samples from the LTSP and collection of 50 additional samples (Appendix B).
- Interpretation of high-resolution seismic-reflection profiles acquired in 2008 and 2009 (Appendix H) and seismic-reflection profiles from the LTSP (PG&E, 1988).
- Analysis of magnetic-field data from helicopter and ship-born measurements (Appendix D).
- Evaluation of the earthquakes associated with the Shoreline seismicity lineament (Section 4.2).

This section describes the location, length, faulting style, dip, activity, slip rate and relationship of the Shoreline fault zone to other faults in the region. The Shoreline fault zone is presented in its entirety on Plate 1 at 1:35,000 scale. Several comparative maps illustrate the interpretations of geology and submerged marine terraces with the MBES bathymetric imagery along the N40W fault and the Central and South segments of the Shoreline fault zone at key locations at a more detailed 1:12,000 scale. These comparative maps highlight the following areas: (1) west of Lion Rock, (2) directly west of DCPP, (3) directly south of DCPP, (4) southwest of Olson Hill, (5) west of Rattlesnake Creek, and (6) southwest of Point San Luis (Figures 4-9 to 4-15). In this

section, the alternative interpretations and uncertainties in the fault characteristics are explicitly discussed to provide the rationale for establishing the range of fault parameters in the logic tree characterization presented in Section 5.

The Shoreline fault zone appears to be a locally reactivated preexisting fault. Although the preexisting fault is not reflected in the regional gravity data (Figure 4-16), this older fault is associated with a distinct, linear magnetic anomaly as seen in the high-resolution helicopter magnetic field data (Appendix D and Figure 4-17). The magnetic field associated with the older fault zone is probably from serpentinite or greenstone lenses within Franciscan mélange along the portion of the fault between about Olson Hill and offshore Point San Luis (Figure 4-18). Juxtaposition of magnetic (e.g., greenstone) against nonmagnetic (e.g., sandstone) blocks of pre-Tertiary rock along the older fault zone accounts for the strong contrast in the magnetic field strength. The prior episode of faulting dates to late Miocene and perhaps Pliocene time that probably occurred either during a regionally recognized mid-Miocene to early Pliocene period of transtensional deformation or during a later middle to late Pliocene period of transpressional deformation (PG&E, 1988 and references therein).

The current transpressional deformation regime began in about the middle Pliocene, coincident with reorganization of the Pacific-North America plate boundary (Lettis et al., 2004 and references therein). This reactivated several faults bounding the Irish Hills and the rest of the San Luis Range. Since one to two million years ago, the mode of deformation in the Irish Hills switched from folding to block uplift (Lettis et al., 2004; Hanson et al. 1994). Some but not all of the structures active during the earlier episodes of faulting have been reactivated in the current tectonic regime. Quaternary erosion during periods of lower sea level or during transgressions to sea-level highstands has enhanced the geomorphic expression of preexisting faults formed during the prior episodes of faulting, producing a prominent series of bathymetric lineaments and associated scarps. For example, the prominent escarpment off the coast of Point Buchon that coincides with the N40W fault (Appendix B; Plate 1) appears to be the result of differential erosion rather than late Pleistocene faulting (Section 4.4.2).

The South and Central sublineaments of the Shoreline seismicity lineament align with sections of the preexisting Tertiary fault (within the 0.5 km resolution of the epicenters), indicating that the older fault has been locally reactivated in the current stress regime. Seismicity along the Northern sublineament, however, trends northwest toward the Hosgri fault zone and lies west of the N40W fault (Plate 1). Late Quaternary marine deposits and ephemeral drifting sand sheets on the seafloor mask any geomorphic expression of a fault and any direct surface observation of geologic structure that may be associated with the Northern seismicity sublineament. The origin of the Northern seismicity sublineament and direct linkage to a bedrock fault, therefore, is less certain than for the Central and Southern sublineaments of the seismicity trend. As described in Section 4.2.4, alternative structural origins of the Northern seismicity sublineament include (1) a steeply east-dipping Hosgri fault zone; (2) a subvertical fault (buried or emergent) coincident with the seismicity sublineament; and (3) the N40W fault, with a steeply west-dipping shallow crustal portion to link the surface trace of the fault with the seismicity trend. As discussed in Section 4.2.4, the analysis of the seismicity is the basis for preferring the subvertical fault model.

Three methods are used to evaluate whether a direct structural link can be made between the Hosgri fault zone and a distinct causative fault associated with the Northern seismicity sublineament:

1. Reexamination of the USGS high-resolution seismic-reflection profiles that cross the Northern seismicity sublineament.
2. Reprocessing of three of these high-resolution seismic-reflection profiles to improve data resolution.
3. Reexamination of 1980s-era high-energy Comap CDP seismic-reflection profiles interpreted during the LTSP (PG&E, 1990) that cross the Northern seismicity sublineament and the N40W fault trend.

Reexamination of an earlier Comap CDP seismic-reflection profile (CM-21) collected across the northern end of the Northern seismicity sublineament reveals gently folded Tertiary strata east of the Hosgri fault zone with no evidence of faulting across the Northern seismicity sublineament to the limit of the resolution of the Comap data (Figure 4-19). In contrast, this Comap seismic-reflection profile shows disruptions in reflectors consistent with faulting or tight folding across the nearby N40W fault.

Reprocessed high-resolution seismic-reflection profiles at the northern and southern ends of the Northern seismicity sublineament provide significant improvement in overall data clarity compared to the basic processing by the USGS. Although the seismic-reflection data are still insufficient to resolve definitively the presence or absence of faulting, careful reexamination of the high-resolution profiles crossing the central portion of the Northern seismicity sublineament permits an interpretation of minor vertical separations across subvertical faults in Tertiary strata that are plotted on Plate 1 as two concealed, queried, en echelon faults. The southwestern fault follows the axis of a well-expressed syncline in Tertiary strata and the fault to the northeast is subparallel to the syncline. These faults generally align with the Northern seismicity sublineament. Preliminary estimates of vertical separations are on the order of 5–10 m with the northeast side down. This is opposite to the direction of Quaternary uplift of the Irish Hills. Direct correlation of Tertiary strata across the faults also suggests that the amount of cumulative lateral displacement is also limited to a few tens of meters or less. These faults clearly lie west of the N40W fault, and are named the North segment of the Shoreline fault (Plate 1). Given the minor displacement of Tertiary strata, the North segment of the Shoreline fault zone does not appear to be associated with a well-developed older Tertiary fault similar to the Central and South segments of the Shoreline fault zone.

Based on the above evidence, three alternative interpretations of the North segment of the Shoreline fault zone are considered. The preferred alternative is that the North segment of the Shoreline fault zone coincides generally with the Northern seismicity sublineament as shown on Plate 1. The fault either has produced only minor displacement in the Tertiary strata in the near surface or does not extend to the seafloor (i.e., is not emergent). This location for the fault is preferred because it most closely aligns with the Northern seismicity sublineament. The second alternative locates the North segment along the N40W fault. This alternative is less preferred because the N40W fault departs from the strike of the seismicity lineament, but the N40W fault is a recognized preexisting fault that is associated with microseismicity along its southeastern

trend (i.e., the Central and South segments). The third alternative is that some or all of the Northern seismicity sublineament is associated with an east-dipping Hosgri fault zone, in which case the North segment of the Shoreline fault zone does not exist or is limited to a few kilometers in length beyond the better-defined Central segment. These alternatives and their potential significance to hazard are discussed further in Section 5.

4.3.1 Length and Segments

The Shoreline fault zone, including all three segments, has an overall strike of about N60°W and is up to 23 km long (Plate 1). The total length of individual segments and the continuity and integration of the fault as a whole are discussed in the following subsections.

North Segment

The North segment is up to 8 km long. The uncertainty in the segment length encompasses the range of alternative locations described above ranging between zero length (with seismicity occurring on an east-dipping Hosgri fault zone at depth) and the maximum 8 km length extending southeast from the Hosgri fault zone to south of Lion Rock. The alternative N40W fault trace also yields an 8 km segment length. The North segment is concealed beneath marine sediments and the ephemeral drifting sand sheet on the seafloor, and has no geomorphic expression. The alternative surface trace along the older N40W fault coincides with the mapped trace west of Lion Rock and the linear escarpment accented by erosion that created a composite series of submerged marine strandlines across the fault (Appendix I). West of Lion Rock a late Pleistocene submerged wave-cut platform extends across the N40W fault with no apparent vertical separation within a limit of resolution of 1 m (Figure 4-9).

The two alternative locations of the North segment have different expressions in the magnetic field data (Figure 4-17). The preferred trace that follows the seismicity sublineament does not coincide with a strong magnetic anomaly, although the lack of an anomaly may simply reflect progressively deeper seawater and Quaternary sediments along this trace of the fault. The alternative N40W trace is subparallel to but crosses a magnetic anomaly associated with intrusive diabase (Figure 4-17; Appendix B). The south ends of both the North segment and the N40W fault are obscured by sand sheets, so the connection between the North and Central segments is unclear. The anomalies in the magnetic-field data are not continuous and appear complex; this complexity in the magnetic-field data indicates probable structural complexity at this segment boundary.

Central Segment

The Central segment is approximately 8 km long and follows an older reactivated Tertiary fault that is well expressed in the geology and as a magnetic anomaly (Plate 1; Figure 4-17). The Central segment is further divided into three en echelon subsegments, C-1, C-2, and C-3. These subsegments are not considered to be rupture segments in the seismic source characterization of the Shoreline fault zone (Section 5). Subsegment C-1 merges with a strike change with C-2, and C-2 has a right step to C-3 of 100–200 m. Subsegment C-1 is west of Discharge Cove and appears to die out northward beneath the sand sheet directly south of Lion Rock. The northern end of C-1, however, does not follow the magnetic anomaly high that characterizes the majority of the Central and South segments but transitions into a magnetic trough. Subsegment C-1

forms a very prominent and well-defined bathymetric lineament and, where mapped at the seafloor, juxtaposes Tertiary diabase against Franciscan mélange (Figure 4-10).

Subsegment C-2 also forms a very prominent, well-defined bathymetric lineament and juxtaposes Obispo diabase, Cretaceous sandstone and Franciscan mélange on the east against a thin mobile sand sheet covering Franciscan mélange on the west (Figure 4-11). West of Olson Hill, a moderate to strong, 900 m long geomorphic lineament is evident on the MBES bathymetric image. The lineament lies within a shallow, 2–4 m-deep, 25 m-wide trough in Franciscan mélange and is likely accentuated by differential erosion (Figure 4-12). In this area of subsegment C-2, two small pockmarks in a mobile sand sheet are well expressed on the 2009 bathymetry, but are absent on the 2010 bathymetry (Figure 4-12). If these pockmarks are not data artifacts but are formed by gas or fluid expulsed along the fault zone, their disappearance in the 2010 bathymetry illustrates the mobile, ephemeral nature of the sand deposits that locally veneer the seafloor.

The subsegment C-2 coincides with a linear magnetic anomaly high (Figures 4-17 and 4-18). To the south, subsegment C-2 ends near where the Olson Hill deformation zone (the northern splay of the San Luis Bay fault zone) projects offshore. A direct structural or geomorphic linkage between the Central segment of the Shoreline fault zone and the bedrock faults near Olson Hill has not been established (Figure 4-13). The step-over between subsegments C-2 and C-3 is southeast of Olson Hill where the linear, magnetic anomaly high ends.

Subsegment C-3 also is expressed as a well-defined bathymetric lineament (Plate 1; Figure 4-14). The lineament is primarily in Cretaceous sandstone and Franciscan mélange and is covered by a thin sand sheet. The lineament coincides with a magnetic anomaly high (Figure 4-18). As shown on Figure 4-14, the southern end of subsegment C-3 may bend to the east and follow a lineament (also interpreted to be a paleostrandline) that projects directly toward the Rattlesnake fault (the southern strand of the San Luis Bay fault zone) at the coastline. The apparent connection of the two faults suggests that there may be a kinematic link between these two structures, but analysis of the submerged wave-cut platform associated with the marine oxygen isotope stage (MIS) 5a sea-level highstand (approximately 80,000 years old) indicates that the Shoreline fault zone is probably a separate structure (Appendix I). Alternatively, the south end of the Central segment may continue on strike beneath the mobile sand sheet to the southeast toward a linear magnetic high before ending within a kilometer or so.

South Segment

The South segment is approximately 7 km long and, like the Central segment, follows a reactivated older bedrock fault. It is expressed as a poor to moderate bathymetric lineament inferred to be in a band of mélange covered by a thin mobile sand sheet. Locally, the South segment truncates bedding in Cretaceous sandstone along a low, northeast-facing escarpment (Plate 1; Figure 4-15). It is also associated with a strong linear magnetic anomaly high (Figure 4-18). In detail, the fault trace defined on the MBES bathymetry image follows the west flank of the magnetic high rather than the crest. The northern end of the South segment lies within a broad zone of Franciscan mélange that is covered by a sand sheet, so its exact location is uncertain. The junction between the Central and South segments is interpreted as either a right step-over of 100–500 m, or the two segments meet at the north end of the linear magnetic

anomaly southeast of Rattlesnake Creek. The south end of the South segment projects beneath a sand sheet southwest of Point San Luis and southwest of the southern cluster of seismicity that marks the south end of the Southern seismicity sublineament (Plate 1; Figure 4-1).

4.3.2 Faulting Style

The Shoreline fault zone is inferred to be primarily a right-lateral fault based on focal mechanisms that indicate vertical strike-slip fault motion (Figure 4-7) and the linear geologic expression of the fault on the seafloor along the Central and South segments. However, some focal mechanisms along the North and Central segments show right-oblique or right-reverse motion, and one focal mechanism along the South segment shows right-normal motion. These oblique mechanisms suggest that the fault may accommodate some vertical displacement as well as lateral displacement. However, as discussed in Section 4.4, the vertical component of displacement along the Shoreline fault zone is less than approximately 2 m on submerged wave-cut platforms estimated to be 75,000 years old or older (Figures 4-10, 4-11, 4-13, 4-15, 4-24, and 4-25). These data support a characterization of the Shoreline fault zone as a strike-slip fault with a limited vertical component.

4.3.3 Geometry and Downdip Width

The seismicity defines a nearly vertical fault zone (Figures 4-2 and 4-8). Along the Central and Southern seismicity sublineaments, the hypocentral distribution of seismicity forms a nearly vertical alignment to a depth of about 8–10 km. The vertical alignment of seismicity is consistent with the results of the 2-D magnetic profile modeling discussed in Appendix D. The magnetic data along a southwest-northeast cross section passing south of Olson Hill indicate that the source body associated with the Shoreline fault zone is nearly vertical, with a width on the order of 200 m, and extends from the near-surface to a depth ranging from several hundred meters to several kilometers below the surface (Figure 4-20)

Along the northern seismicity sublineament, the seismicity is more diffuse and forms a nearly vertical alignment to a depth of about 12–15 km. Steep dips for magnetic source bodies along the Northern seismicity lineament are not as well constrained as the Central and Southern sublineaments due to the possible effects of deep water relative to the survey flight elevation (Appendix D). As discussed previously, it is not certain how much of the seismicity along the Northern seismicity sublineament, in particular the deeper seismicity, may be associated with a steeply east-dipping Hosgri fault zone.

4.4 Activity of the Shoreline Fault Zone

Several approaches are used for assessing the recency of activity and the slip rate of the Shoreline fault zone as discussed below. Of primary importance are the identification and dating of offshore late Quaternary marine terraces, which consist of submerged paleostrandlines (ancient shorelines) and associated wave-cut platforms. These are discussed in Section 4.4.1. The geometries and distribution of offshore marine terrace (e.g. Hanson et al., 1994), including direct measurements of late Quaternary vertical separation across the Shoreline fault zone and N40W fault. The assessment of recency of activity and slip rate are discussed in Sections 4.4.2 and 4.4.3, respectively.

4.4.1 Offshore Wave-Cut Platforms and Paleostrandlines

A detailed analysis of ancient offshore marine terraces was performed in the study area (Appendix I, Figure 4-21). The recently acquired high-resolution MBES bathymetric data and USGS high-resolution seismic-reflection profiles allowed the identification and mapping of the submerged marine wave-cut platforms and paleostrandlines. The interpretation of these submerged geomorphic features helped constrain the location and rates of deformation along the Shoreline fault zone and the surrounding continental shelf. The submerged marine terraces were mapped in the entire offshore bedrock platform extending from the coastline between Estero Bay and San Luis Obispo Bay west to the Hosgri fault zone. Results of the study are presented in detail in Appendix I and briefly summarized below.

The offshore marine terraces contain two spatially distinct terrace sequences on the inner continental shelf: one sequence is on the Islay shelf west of Point Buchon and the other sequence is on the Santa Rosa Reef shelf west of Point San Luis (Figure 4-21). The terraces appear to correlate laterally within each shelf, but do not appear to correlate between the two shelves. The submerged terraces on these shelves have not been independently dated, but analysis of possible periods of formation (Appendix I) shows that they are older than the last glacial maximum (LGM) that occurred about 22,000 years ago. The preferred interpretation is that the marine terrace sequence on the Islay shelf is the offshore continuation of the onshore flight of emergent marine terraces near Point Buchon (and are being uplifted at a rate of 0.2 mm/yr; Hanson et al., 1994), and the marine terrace sequence on the Santa Rosa Reef shelf is the offshore continuation of the onshore flight of emergent marine terraces at Point San Luis (and are being uplifted at a rate of 0.06 mm/yr; Hanson et al., 1994). Using this model, the shallower offshore marine terraces generally correlate to MIS 5 stillstand sea levels of approximately 75,000 to 100,000 years ago, and the deeper marine terraces are older than the LGM that occurred about 22,000 years ago and generally correlate to MIS 3 stillstand sea levels approximately 30,000 to 50,000 years ago. Some of the wave-cut platforms on the Islay and Santa Rosa Reef shelves are probably reoccupied and modified from wave-cut platforms developed during stillstand sea levels that occurred prior to the last interglacial (MIS stage 5e; approximately 120,000 years ago).

The submerged paleostrandlines and associated wave-cut platforms have been modified by the last marine transgression, but as discussed in detail in Appendix I, the extent of the modifications are relatively minor and localized. Given the relatively rapid rise in sea level and because the zone of wave erosion (approximately 10–15 m deep) past any one place on the shelf within a period of 1,000–1,500 years, no wave-cut platforms wider that approximately 100 m could have formed, and vertical lowering of the platform is limited to about 1–1.5 m (Appendix I, Sections 7.2.1.2 and 7.2.1.3). Therefore, while wave erosion during the last marine transgression may have locally removed some geomorphic evidence of recent faulting, if present, it would not destroy larger vertical offsets (on the order of multiple meters) or remove significant geomorphic evidence of extensive late Quaternary faulting over the entire reach of the Shoreline fault zone.

Based on the above observations, the submerged wave-cut platforms and paleostrandlines older than about 75,000 years (i.e., Stage 5 stillstands) constrain the rate of vertical separation across the Central and South segments of the Shoreline fault zone and N40W fault (discussed in 4.4.3

below). The Islay and Santa Rosa Reef terrace sequences are separated by a change in uplift rate that occurs in a poorly defined zone that lies west of the Shoreline fault zone.

4.4.2 Evidence of Activity

The seismicity along the Central and Southern sublineaments aligns with the Central and South segments of the Shoreline fault zone within the 0.5 km horizontal uncertainty (Plate 1**,** Figure 4-1). Because of this direct association with seismicity, PG&E concludes that the Central and South segments of the Shoreline fault zone are active, and infers that the Northern seismicity sublineament is part of the active fault zone. The alternative and less preferable interpretation that the seismicity of the Northern seismicity sublineament may be wholly or in part produced by the Hosgri fault zone is also acknowledged.

No definitive evidence of late-Quaternary displacement has been observed anywhere along the Shoreline fault zone or the N40W fault. Elevation profiles on the late Quaternary wave-cut platforms across the N40W fault and Central and South segments of the Shoreline fault zone do not show systematic vertical separation across the faults (Section 4.4.3 and Figures 4-9, 4-11, and 4-15). The moderate to strong geomorphic lineament in bedrock west of Olson Hill is interpreted to be formed by differential erosion (Section 4.3.1 and Figure 4-12). Similarly, the small scarp and associated geomorphic features imaged in the high-resolution seismic-reflection profiles off Intake Cove (Figure 4-10) are interpreted to be formed by differential erosion (Appendices B and I).

4.4.3 Slip Rate

The Shoreline fault zone lies entirely offshore and thus it is difficult to develop direct quantitative estimates of slip rate. The MBES bathymetric data were extensively probed to identify piercing points (i.e., potentially datable geomorphic features such as paleostrandlines or submerged channels on both sides of the fault zone that could be used to constrain cumulative lateral slip and slip rate). No geomorphic features that could be reliably used as lateral offset markers have been identified. In the absence of more direct information, constraints on slip rate are provided by several qualitative and indirect quantitative estimates of slip rate. These are summarized below.

Comparison to the Hosgri–San Simeon Fault System

The Hosgri–San Simeon fault system has a slip rate of 0.5 to 6 mm/yr, with a preferred rate of 1 to 3 mm/yr (Hall et al., 1994; Hanson et al, 1994; Hanson et al., 2004). Onshore, the San Simeon fault is well expressed geomorphically and clearly displaces late Pleistocene and Holocene deposits at numerous locations. Offshore, the Hosgri fault zone locally produces scarps on the seafloor and, along the reach of the fault directly west of the Irish Hills, abruptly truncates the westward extent of the offshore bedrock platform. In addition, individual strands of the Hosgri fault zone produce linear escarpments in bedrock that appear to be pressure ridges on the seafloor. All of these features on the Hosgri fault zone occur in water depths shallower than 120 m, and thus, if present at the time of the last transgression, were subject to erosion. The Shoreline fault zone is not associated with geomorphic or geologic features similar to those of the Hosgri fault zone offshore or the San Simeon fault zone onshore. Geomorphic features produced by high slip rate faults are lacking, even in locations where the fault zone extends into deeper water where the relatively rapid rise in sea level during the last sea-level transgression

caused sea level to pass more rapidly than in shallow water, shortening the duration that potential fault features would have been exposed to wave erosion, and reducing the likelihood that they would have been significantly eroded (Appendix I).

In addition, if the Shoreline fault zone had a slip rate comparable to the Hosgri–San Simeon fault system, it is likely that it would be part of a longer fault zone with an onshore portion along strike to the southeast (for example, it would likely be a part of a longer and more active Southwestern Boundary fault zone). If this were the case, it would be expected that the Shoreline fault zone would have maintained a seafloor expression southwest of Point San Luis, and evidence of higher slip rate faults in the associated Southwestern Boundary zone would be expressed onshore in the vicinity of San Luis Obispo Bay or the Santa Maria Valley. Despite extensive onshore mapping in this area during both the LTSP and during this study, no onshore faults with comparable geomorphic expression to the San Simeon fault have been identified.

Based on these observations, the slip rate on the Shoreline fault zone is qualitatively estimated to be at least an order of magnitude less that the slip rate on the Hosgri–San Simeon fault zone. This qualitative comparison yields an estimate of horizontal slip rate of 0.05 to 0.6 mm/yr for the Shoreline fault zone.

Estimates of Vertical Separation

Two approaches are used to constrain the amount of vertical separation on the Shoreline fault zone. Along the North segment (associated with the Northern seismicity sublineament), possible displaced Tertiary strata on high-resolution seismic-reflection profiles are interpreted to constrain the cumulative amount of vertical separation on the segment to be about 5–10 m, with a northeast-side down vertical separation. The northeast-side down sense of vertical separation is opposite the expected northeast-side up vertical separation if the fault is partially accommodating uplift of the San Luis–Pismo block. In addition to the apparent limited vertical stratigraphic separation, the similarity in the seismic stratigraphy across the fault zone observed at these two locations probably indicates limited lateral displacement as well. These interpreted faults are similar to several small displacement faults imaged in the MBES bathymetric data that are associated with folds in the Monterey and Pismo Formations west of Point Buchon that probably formed in the Miocene and early Pliocene (Plate 1). However, estimating an onset of deformation at between 1 and 2 million years ago (coinciding with the estimated onset of block uplift recorded by emergent marine terraces on the adjacent coast; Hanson et al., 1994) the vertical separation rate would be less than 0.01 mm/yr.

The second approach to constrain vertical separation rates across the Shoreline fault zone is based on the evaluation of submerged wave-cut platforms that are mapped across the N40W fault and Central and South segments of the fault zone (Appendices B and I). The amounts and estimated rates of vertical separation of wide wave-cut platforms across mapped faults are constrained at the following locations (from north to south):

- The wave-cut platform associated with the –38 m paleostrandline crosses the N40W fault west of Lion Rock (Figure 4-9). The probable timing of the most recent sea-level occupation (and associated significant geomorphic modification of the –38 m paleostrandline on the Islay shelf) was between 49,000 and 60,000 years ago (Appendix

I). Analysis of elevation profiles across the wave-cut platform suggests that there is zero vertical separation across the mapped fault trace with a combined uncertainty of approximately ±2 m (Appendix I, Section 7.3.1). This limits the maximum vertical separation rate across the N40W fault to less than 0.04 mm/yr.

- The wave-cut platform associated with the –25 m paleostrandline crosses the C-1 subsegment of the Central segment of the Shoreline fault zone west of DCPP (Figure 4-10). The estimated vertical separation of the buried wave-cut platform associated with the –25 m paleoshoreline in the step-over region between the C-1 and C-2 subsegments of the Shoreline fault zone is either 0 (from the preferred interpretation that the apparent scarp is due to differential erosion) or 1 ± 2.5 m with the center value having a northeast-side up vertical separation (Appendix I, Section 7.3.2). Using the vertical separation and the estimated minimum age of 75,000 years for the wave-cut platform yields a vertical separation rate of 0 or 0.01 ± 0.03 mm/yr.
- The wave-cut platform associated with the –21 m shoreline crosses the C-2 subsegment of the Central segment of the Shoreline fault zone (Figure 4-11). The –21 m paleostrandline and wave-cut platform are also estimated to be at least 75,000 years old. Analysis of elevation profiles across the wave-cut platform suggests there is zero vertical separation across the mapped fault trace with a combined uncertainty of approximately ±1.5 m (Appendix I, Section 7.3.2), the upper bound of 1.5 m of vertical deformation across the mapped fault trace limits the vertical slip rate to be less than 0.02 mm/yr.
- The wave-cut platform associated with the –31 m paleostrantline crosses the South segment of the Shoreline fault zone near its south end (Figure 4-15). The platform and associated paleostrandline (also estimated to be at least 75,000 years old) extend across the fault zone. Analysis of elevation profiles across the wave-cut platform suggests there is zero vertical separation across the mapped fault trace with a combined uncertainty of approximately ± 1.5 m (Appendix I, Section 7.3.3), constraining the upper bound to be about 1.5 m. This limits the vertical slip rate to less than 0.02 mm/yr.

The results summarized above suggest that the vertical separation rate on the Shoreline fault zone is indistinguishable from zero. In order to estimate a maximum horizontal slip rate from the wave-cut platform data, the maximum vertical separation rates are considered with a fault having an assumed 10:1 horizontal-to-vertical slip ratio. This assumption yields maximum horizontal slip rates on the order of 0.2 to 0.4 mm/yr.

Estimates of Cumulative Right-Lateral Strike-Slip

Toward the northern end of the Central segment of the Shoreline fault zone, directly west of Discharge Cove, two west-northwest-trending, subparallel magnetic anomaly highs show an apparent right-lateral step of about 300 m (Figure 4-22). Although not a unique interpretation, the apparent right-lateral step may occur across a N15ºE striking basement fault whose north end aligns with the north-south to N25ºW striking fault mapped in the headland at the northwest end of Discharge Cove. This fault, which is referred to as the N15E fault, may cross the Central segment of the Shoreline fault zone. Thus, the N15E fault provides a possible piercing line or strain gauge from which cumulative right-lateral displacement on the Shoreline fault zone can be estimated.

The N15E fault, where mapped onshore and in the rocks at low tide, juxtaposes resistant Obispo Formation tuff against Obispo Formation bedded sedimentary rock in a broad zone of shearing that is associated with hydrothermal alteration. The N15E fault is truncated to the north by an east-west-striking fault that is clearly mapped in the intertidal zone and in the sea cliff (Plate 1**;** Figure 4-22). This east-west fault does not displace the emergent MIS 5a (approximately 80,000 years old) wave-cut platform exposed in the sea cliff, and illustrates the inactivity of the N15E fault. The inferred right-lateral separation of the magnetic anomalies across the N15E fault is supported by the right-lateral separation of other approximately north-south-striking faults mapped elsewhere in the vicinity of DCPP (Appendix B).

Alternative traces of the N15E fault through the MBES bathymetric data that satisfy the right-lateral separation of the twin magnetic anomaly peaks are shown on Figure 4-22. The alternative traces limit the possible offset of the N15E fault across the Central segment of the Shoreline fault zone to less than 100–200 m right-lateral, and possibly zero (Figure 4-22). Estimating an onset of deformation at between 1 and 2 million years ago (coinciding with the estimated onset of block uplift recorded by emergent marine terraces on the adjacent coast; Hanson et al., 1994) yields an estimated maximum horizontal dextral slip rate of about 0.05 to 0.2 mm/yr for the Shoreline fault zone.

Seismicity

The rate of seismicity on the Shoreline seismicity lineament provides a limited constraint on the slip rate on the Shoreline fault zone. Figure 4-3c shows the maximum likelihood fit of the Shoreline seismicity (empirical fit) in comparison to mean characteristic recurrence models for characteristic magnitudes of 5.8 (single segment rupture), 6.0 (two segment rupture) and 6.5 (total fault rupture) using the qualitative slip rates of 0.01 and 0.3 mm/yr reported in the Progress Report (PG&E, 2010a). The Shoreline seismicity rate is most consistent with the recurrence model having a mean characteristic magnitude 5.8 earthquake (single segment rupture) with a slip rate of 0.3 mm/yr rather than the lower slip rate of 0.01mm/yr. Extrapolating the slope of the empirical data based on a *b*-value of 0.93 out to M 6.0 results in an estimated annual recurrence of about 0.0002 events/yr and a return period of about 5,000 yrs.

San Luis Bay Fault Zone

An alternative structural interpretation of the Shoreline fault zone is that it is kinematically linked to the San Luis Bay fault zone such that the slip on the North and Central segments of the Shoreline fault zone continues onshore and follows the Rattlesnake fault of the San Luis Bay fault zone and forms part of a strike-slip restraining bend (Plate 1; Figure 4-14). In characterizations based on this linked structural model the slip rate on the San Luis Bay fault zone can be used to provide information on the slip rate of the Shoreline fault zone. The San Luis Bay fault zone has a cumulative rate of vertical separation of 0.14 mm/yr as recorded in the emergent marine terraces at the coast, with about half of that vertical rate occurring on the Rattlesnake fault (PG&E, 1990; Hanson et al., 1994). In addition, detailed mapping along the coastline shows steeply (approximately 70 degrees) north-dipping beds of Cretaceous sandstone and siltstone across the Rattlesnake fault (Figure 4-25).

Tentative correlation of an approximately 35–40 m thick sequence of resistant sandstone beds on the modern wave-cut platform across the Rattlesnake fault yields an estimate of about 70 ± 20 m

of apparent right-lateral separation across the fault, indicating that the Rattlesnake fault does not have significant cumulative deformation across it. Because the beds dip steeply to the north, the apparent right-lateral separation is consistent with pure north-side-up dip-slip motion on a vertical fault of about 190 m. Oblique motion of the Rattlesnake fault would yield horizontal displacements of less than approximately 70 m. An estimated onset of deformation of 1 to 2 million years ago and a maximum horizontal displacement of 70 m yields a limiting lateral slip rate of about 0.14 to 0.07 mm/yr. Considered very unlikely, the absolute maximum lateral slip rate on the fault would consider the limiting horizontal offset of 70 m and a minimum age of 120,000 years, the age of the MIS 5e marine terrace that records the offset of the Rattlesnake fault. This extreme maximum lateral slip rate would be about 0.6 mm/yr. Given the roughly equal distribution of vertical separation between the Rattlesnake fault and Olson Hill deformation zone, the lateral slip rate can be assumed to also be equally distributed, giving a cumulative absolute maximum lateral slip rate for the entire San Luis Bay fault zone of 1.2 mm/yr. As described earlier, given the absence of geomorphic expression onshore along the San Luis Bay fault zone similar to the San Simeon fault, a slip rate of over 1 mm/yr is not credible. Thus this analysis is used to conclude that a maximum lateral slip rate of up to 1 mm/yr may branch from the San Luis Bay fault zone onto the Shoreline fault zone.

Conclusion

Given the above five lines of reasoning, slip rate on the Shoreline fault zone is interpreted to range from 0.05 mm/yr to possibly 1 mm/yr, with a preferred range of 0.2 to 0.3 mm/yr. The slip rate could also be zero.

4.5 Relationship to Other Structures

The Shoreline fault zone lies between the active Hosgri fault zone on the west, the Los Osos fault zone on the north and east, and faults of the Southwestern Boundary fault zone on the south and southeast. Three alternatives are considered for the kinematic relationship of the Shoreline fault zone to these nearby structures.

One alternative is that the Shoreline fault zone is an independent strike-slip fault within the San Luis–Pismo structural block. In this model, the Southwestern Boundary fault zone is a system of reverse faults and the Shoreline fault zone is a minor strike-slip fault accommodating differential slip in the hanging wall of the fault zone. Uplift of the San Luis–Pismo block is accommodated by reverse or reverse-oblique slip on both the Los Osos and Southwestern Boundary fault zones and oblique slip on the Hosgri fault zone. This alternative is most consistent with the structural model proposed in the LTSP (PG&E, 1988; Lettis et al., 1994, 2004).

In the second and third alternatives, the Shoreline fault zone is part of the Southwestern Boundary fault zone that borders the southwestern margin of the uplifting San Luis–Pismo structural block. In these alternatives, the Shoreline fault zone is kinematically linked to the San Luis Bay fault zone, and potentially other faults of the Southwestern Boundary fault zone (i.e., Wilmar Avenue, Los Berros, Oceano, Pecho, and Nipomo faults [PG&E, 1988]). In the second alternative, the Shoreline fault zone is a strike-slip fault linked to the Southwestern Boundary fault zone via left-restraining step-overs in a strike-slip fault system. Uplift of the San Luis–Pismo block is accommodated primarily by reverse or oblique slip on the Los Osos fault zone,

oblique slip on the Hosgri fault zone, and possibly transpressional oblique slip on a Southwestern Boundary strike-slip fault zone.

In the third alternative, the Shoreline fault zone is an integral part of a Southwestern Boundary fault zone system of reverse- and oblique-slip faults. In this model, the Shoreline fault zone is kinematically linked to and may be, in part, the offshore continuation of the San Luis Bay fault zone. Uplift of the San Luis–Pismo block is accommodated by the Los Osos fault zone and by oblique slip on the Shoreline fault zone as part of the overall Southwestern Boundary fault zone.

All three alternatives were considered in the logic tree characterization of seismic source parameters for the Shoreline fault zone (Section 5). Alternative one is considered in an "independent" Shoreline fault zone branch, and alternatives two and three are combined into a single "linked" Shoreline fault zone branch.

4.5.1 Independent Shoreline Fault Zone Model

Determining whether the San Luis Bay fault zone is truncated by the Shoreline fault zone or whether it crosses the Shoreline fault zone is important for assessing the relative merits of the alternative kinematic models presented above. In the scenario where the strike-slip Shoreline fault zone is kinematically independent and separate from the reverse-slip San Luis Bay fault zone, the San Luis Bay fault zone may cross the Shoreline fault zone and extend to the Hosgri fault zone to accommodate uplift of the San Luis–Pismo block. Although the exact location and western limit of the San Luis Bay fault zone in the offshore is uncertain, several lines of evidence support the concept that the onshore San Luis Bay fault zone crosses the inner continental shelf west of the Shoreline fault zone as a deformation zone, possibly as a fold. If so, this structural relationship supports an independent Shoreline fault zone.

The first line of evidence comes from the west-northwest trend of bedrock structures (Appendix B) and the subparallel trending magnetic anomaly (Appendix D) in the offshore. Specifically, there is a broad geologic boundary west of Olson Hill in the offshore geologic map (Plate 1) that places Obispo Formation on the south-southwest against pre-Tertiary rocks on the north-northeast. This north-side up structural relief is similar to the sense of displacement across the San Luis Bay fault zone documented by the emergent marine terraces. The west-northwest trending structural grain in the MBES bathymetric data across this zone do not show a throughgoing fault zone at the seafloor, but a south-southwest-facing monoclinal warp or flexure above a blind fault is permissible. A folding style of deformation (as opposed to surface fault offset) would be similar to the broad deformation of the emergent MIS 5e terrace (approximately 120,000 years old) across the Olson Hill deformation zone (PG&E, 1989c). The San Luis Bay fault zone thus may be partially blind at the coastline and offshore with only some strands (such as the Rattlesnake fault) locally intersecting the surface.

The second line of evidence that the San Luis Bay fault zone crosses the Shoreline fault zone comes from the analysis of the MIS 5a (approximately 80,000 years old) marine terrace and wave-cut platform across the San Luis Bay fault zone (Appendix I). The MIS 5a terrace is observed as a deformed emergent terrace onshore across the Olson Hill deformation zone and in the hanging wall (north side) of the Rattlesnake fault (PG&E, 1989c; Hanson et al., 1994). In the offshore, the MIS 5a wave-cut platform is locally reoccupied but recognizable on either side of

the Rattlesnake fault and on the footwall (south) side of the Olson Hill deformation zone (Appendix I, Section 7.1). Analysis of the offshore marine terraces that reoccupy the MIS 5a wave-cut platform west of Rattlesnake Creek indicates that the vertical deformation of the MIS 5e terrace documented onshore across the Rattlesnake fault continues offshore along strike of the Rattlesnake fault (Figures 4-24 and 4-25; Appendix I). The deformation crosses the southern end of the Central segment of the Shoreline fault zone without evidence of displacement on the Central segment.

The third line of evidence for a San Luis Bay fault zone that crosses the Shoreline fault zone comes from the preferred correlation of the paleostrandlines between the Islay and Santa Rosa Reef shelves (Appendix I, Section 7.1). This preferred correlation includes a deformation zone that trends offshore between Diablo Creek and Rattlesnake Creek along the westward continuation of the San Luis Bay fault zone, seaward of the MIS 5a wave-cut platform. Although the specific location of the uplift rate boundary between the Islay and Santa Rosa Reef shelves is not well defined, it is consistent with the general location of the south-southwest-facing monoclinal warp or flexure suggested from the offshore geologic map (first item above).

4.5.2 Linked Shoreline Fault Zone Model

In the alternative models where the Shoreline and San Luis Bay fault zones are kinematically linked as part of the Southwestern Boundary fault zone, one model prediction is that the San Luis Bay fault zone proper may merge with the Shoreline fault zone and will not extend farther west to the Hosgri fault zone. Partial support of this model is the observation that the Rattlesnake fault mapped at the coastline appears to continue offshore as a lineament that merges with the Shoreline fault zone (Plate 1; Figure 4-14). In addition, the uplift rate boundary west of the Shoreline fault zone between the Islay and Santa Rosa Reef shelves is not unique, and thus it is permissible that alternative structures other than a westward continuation of the San Luis Bay fault zone accommodate the differential uplift rate. In the linked fault alternatives listed above, alternative three includes the Shoreline fault zone as a relative uplift rate boundary as part of the margin of the San Luis–Pismo structural block. As described above, our evaluation of submerged marine terraces has documented evidence suggesting a low to zero vertical displacement rate across the Shoreline fault zone (Figures 4-9 to 4-11 and 4-15; Appendix I). This evidence does not support the third alternative wherein the Shoreline fault zone accommodates differential uplift.

4.6 Location of the Shoreline Fault Zone with Respect to DCPP

The mapping based on high-resolution MBES bathymetric data clearly shows a sharp, well-defined lineament that lies offshore and west of the DCPP. This lineament is interpreted as the surface expression of the Shoreline fault zone. Immediately offshore of DCPP, the Central segment of the Shoreline fault zone is located 300 m southwest of the intake structure and 600 m southwest of the power block (Figure 4-10). Onshore geologic mapping documents the absence of late Quaternary deformation within the DCPP site that may be associated with the Shoreline fault zone (Section 7).

Table 4-1 Comparison of Characteristics of the Shoreline Fault Zone presented in the Progress Report (PG&E, 2010a) with this Report

PARAMETER	PROGRESS REPORT (PG&E, 2010a)	THIS REPORT (2011)
FAULT LENGTH	Total Length: 13 to 14 km Two segments: Central and Southern Northern Seismicity Trend considered a separate structure	Total Length: up to 23 km Three segments: North, Central, and South Overall Strike:N60° to 70°W
SEGMENTATION	Three segments w/ lengths (Figure 4-1 this report) Northern Seismicity Trend, 8 to 9 km Central segment, 8 km Southern segment, 5 to 5½ km	Three segments w/ lengths (Figure 4-1 this report): North segment, ~8 km Central segment, ~8 km South segment, ~ 7 km
FAULT DIP	90° based on seismicity	90° based on seismicity and magnetic potential field data
DOWN DIP WIDTH	10 to 15 km from the surface	10 to 15 km from the surface
FAULTING STYLE	Right-lateral strike slip based on linear surface expression of bathymetric lineaments and focal mechanisms.	Right-lateral strike slip based on linear surface expression of bathymetric lineaments and focal mechanisms.
RELATIONSHIP TO OTHER STRUCTURES	Hosgri fault zone (HFZ) • Rupture is inhibited from branching from the HFZ to the Shoreline fault San Luis Bay fault zone (SLBFZ) • Not addressed	Hosgri fault zone (HFZ) • Rupture is inhibited from branching from the HFZ to the Shoreline fault • North Segment dies out before or terminates at the HFZ. • HFZ dips 80 to 85 degrees east, hence some of the deeper seismicity in the North Segment may be on the HFZ San Luis Bay fault zone (SLBFZ) • Relationship to late Quaternary deformation on the SLBFZ uncertain
SLIP RATE	0.01 to 0.3 mm/yr Used Hosgri and San Luis Bay fault zones for comparison	Preferred maximum slip rate: 0.2 to 0.3 mm/yr based on • Comparison with geomorphic/structural expression of the HFZ: 0.05 to 0.6 mm/yr. • Offshore paleo-wave-cut platforms (vertical): <0.02 mm/yr (at 10/1 lateral = < 0.2 mm/yr) • Limited offset of basement fault: 0.05 to 0.2 mm/yr • Seismicity rate: 0.2 to 0.3 mm/yr • Association with SLBFZ: ~0.1 mm/yr
DISTANCE FROM DCPP	600 m southwest of power block 300 m southwest of Intake Structure	600 m southwest of power block 300 m southwest of Intake Structure
SECONDARY DEFORMATION AT DCPP SITE	Negligible Calculation indicates negligible deformation (DCPP.GEO.10.01, R0)	None. Documented absence of late Quaternary primary or secondary surface faulting or other forms of late Quaternary tectonic deformation within the DCPP site that may be associated with a maximum earthquake on the nearby Shoreline fault zone.

Table 4-2a. Absolute and Relative Location Uncertainty Estimates

Analyst	Absolute		Relative	
	Horizontal (km)	**Vertical (km)**	**Horizontal (km)**	**Vertical (km)**
Hardebeck (2010)	0.9	1.3	1.0	0.93
Thurber (2009)	0.5	0.5	0.17	0.28
Waldhauser (2009))	NA	NA	0.2	0.7

Table 4-2b. Average and Median Shifts in Epicenters and Depths between Location Methods for the Shoreline Earthquakes (H=Hardebeck; T=Thurber)

	Horizontal Shifts (km)				**Vertical Shifts (km)**			
	1D vs 3D	**3D vs H-tomoDD**	**1D vs H-tomo DD**	**H-tomoDD vs T-tomoDD**	**1D vs 3D**	**3D vs H-tomoDD**	**1D vs H-tomoDD**	**H-tomoDD vs T-tomoDD**
Median	1.499	0.496	1.045	0.450	0.66	0.302	0.779	1.293
Average	1.469	0.603	1.273	**0.510**	0.880	0.411	1.126	**1.329**
StdDev	0.743	0.381	0.901	0.328	0.761	0.363	0.955	0.842

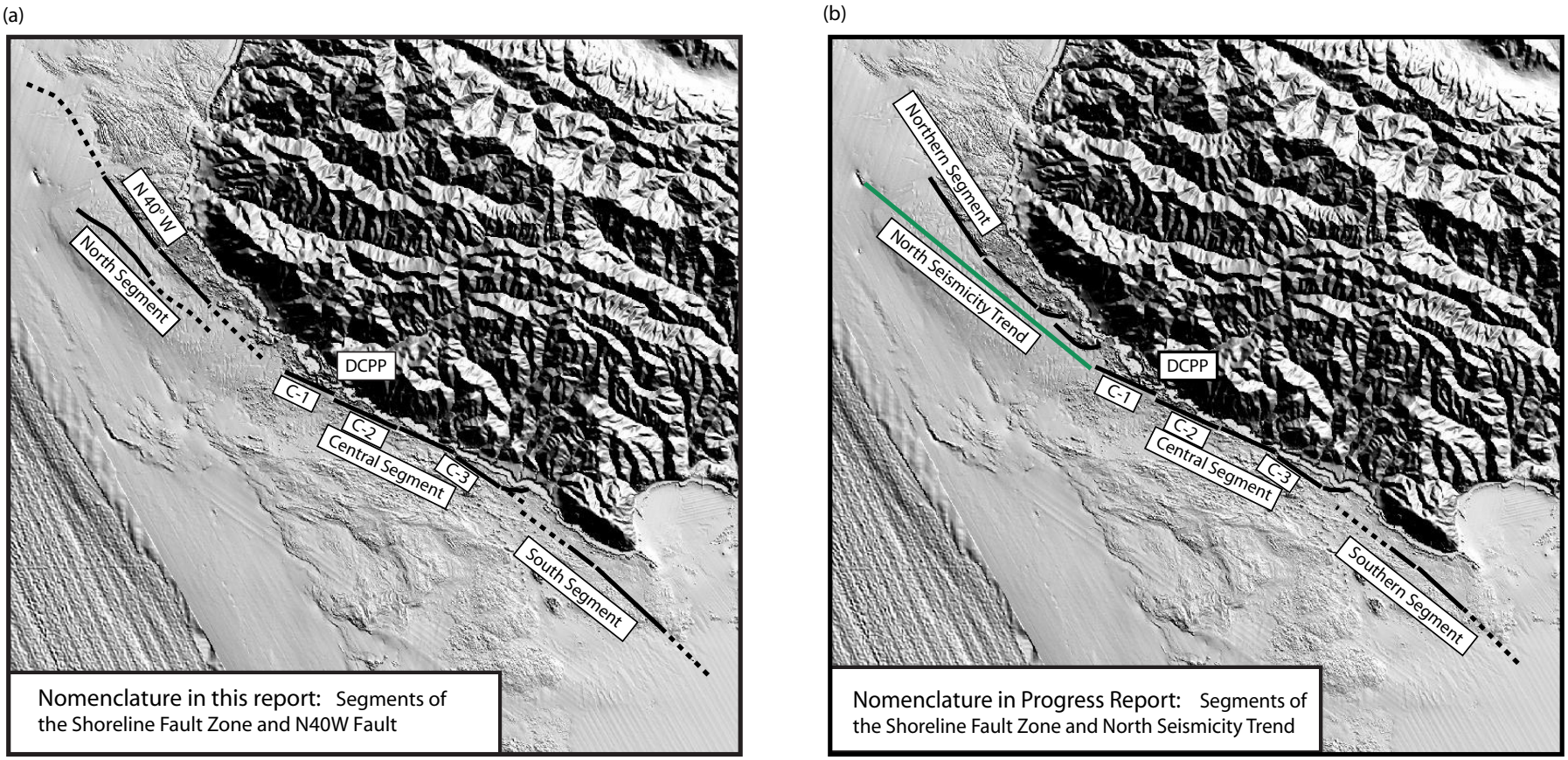

Map projection: NAD 1983, UTM Zone 10 North

0 2.5 5 Miles

0 2.5 5 Kilometers

Comparison of nomenclature for (a) the Shoreline fault zone in this report and (b) the Progress Report (PG&E, 2010a)

SHORELINE FAULT ZONE STUDY

Pacific Gas and Electric Company

Figure **4-1**

File path: S:\13800\13838\13838.002\Figures\20101112_Report\Figure_4-1.ai; Date: [12/21/2010]

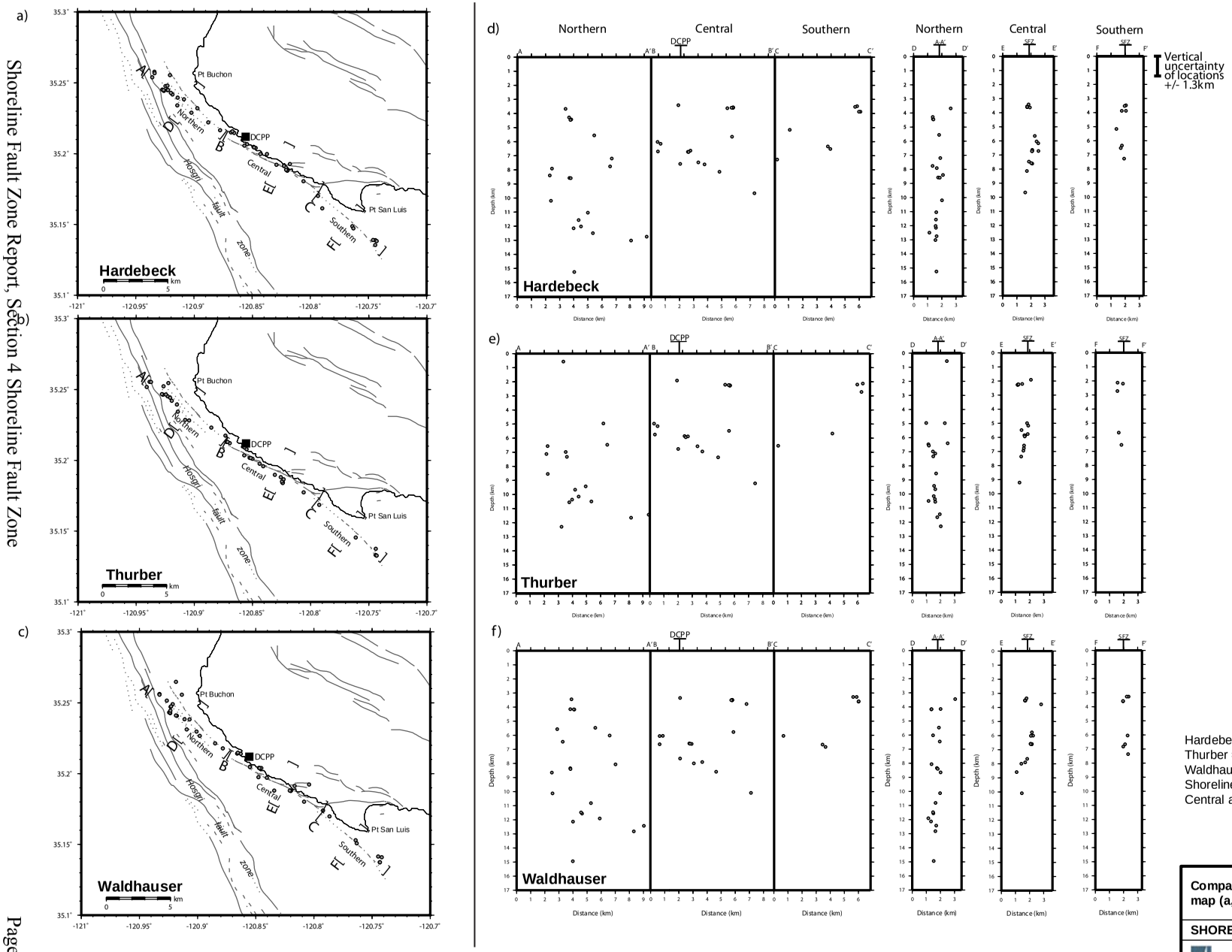

Hardebeck =TomoDD (Hardebeck, 2010), Thurber = TomoDD (Thurber, 2009), Waldhauser= HypoDD (Waldhauser, 2009). Shoreline seismicity sub-lineaments, Northern, Central and Southern, are labeled.

Comparison of shoreline seismicity relocations in map (a, b, c) and cross section (d, e, f) views.

SHORELINE FAULT STUDY

Pacific Gas and Electric Company

Figure **4-2**

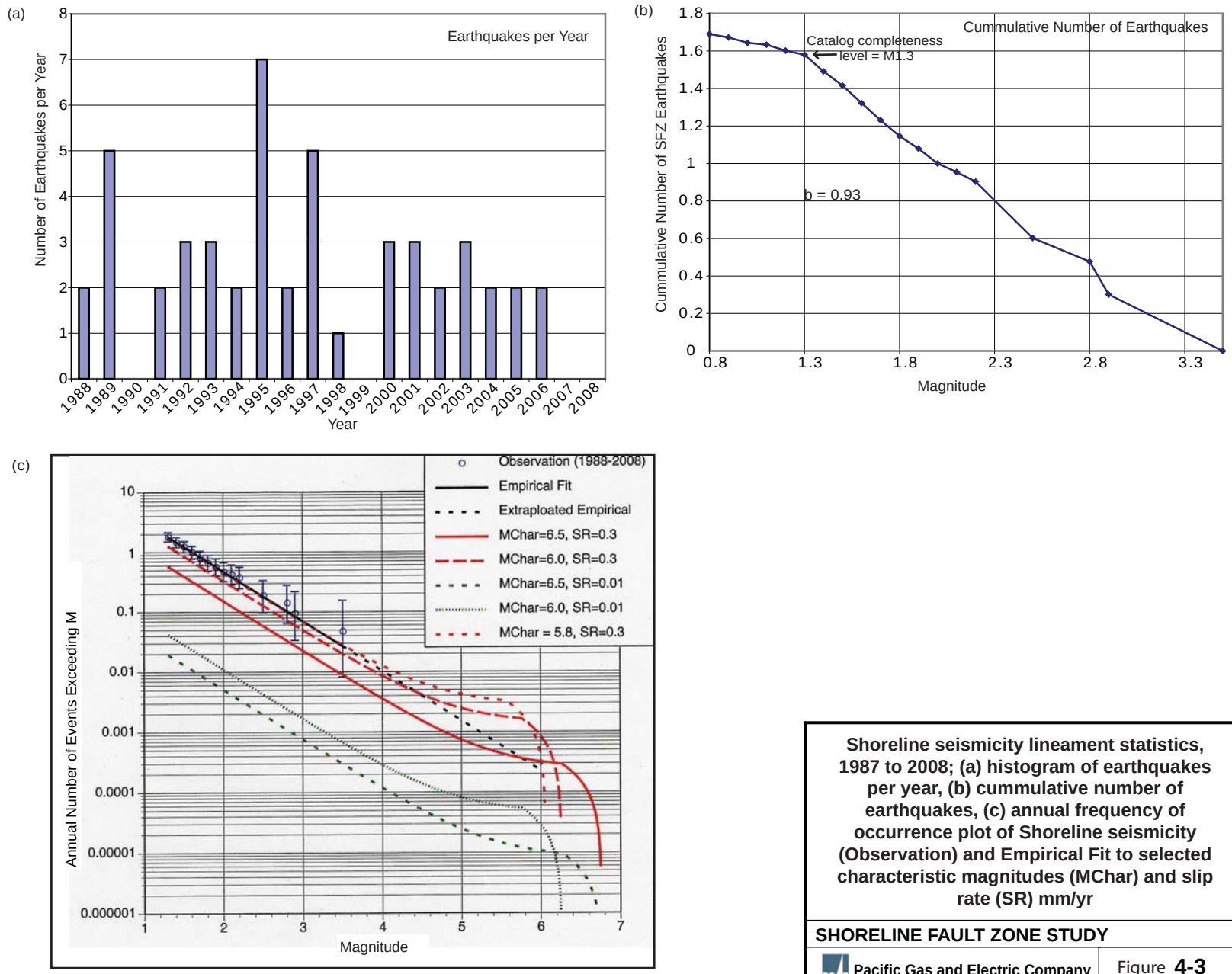

Shoreline seismicity lineament statistics, 1987 to 2008; (a) histogram of earthquakes per year, (b) cummulative number of earthquakes, (c) annual frequency of occurrence plot of Shoreline seismicity (Observation) and Empirical Fit to selected characteristic magnitudes (MChar) and slip rate (SR) mm/yr

SHORELINE FAULT ZONE STUDY

Pacific Gas and Electric Company Figure **4-3**

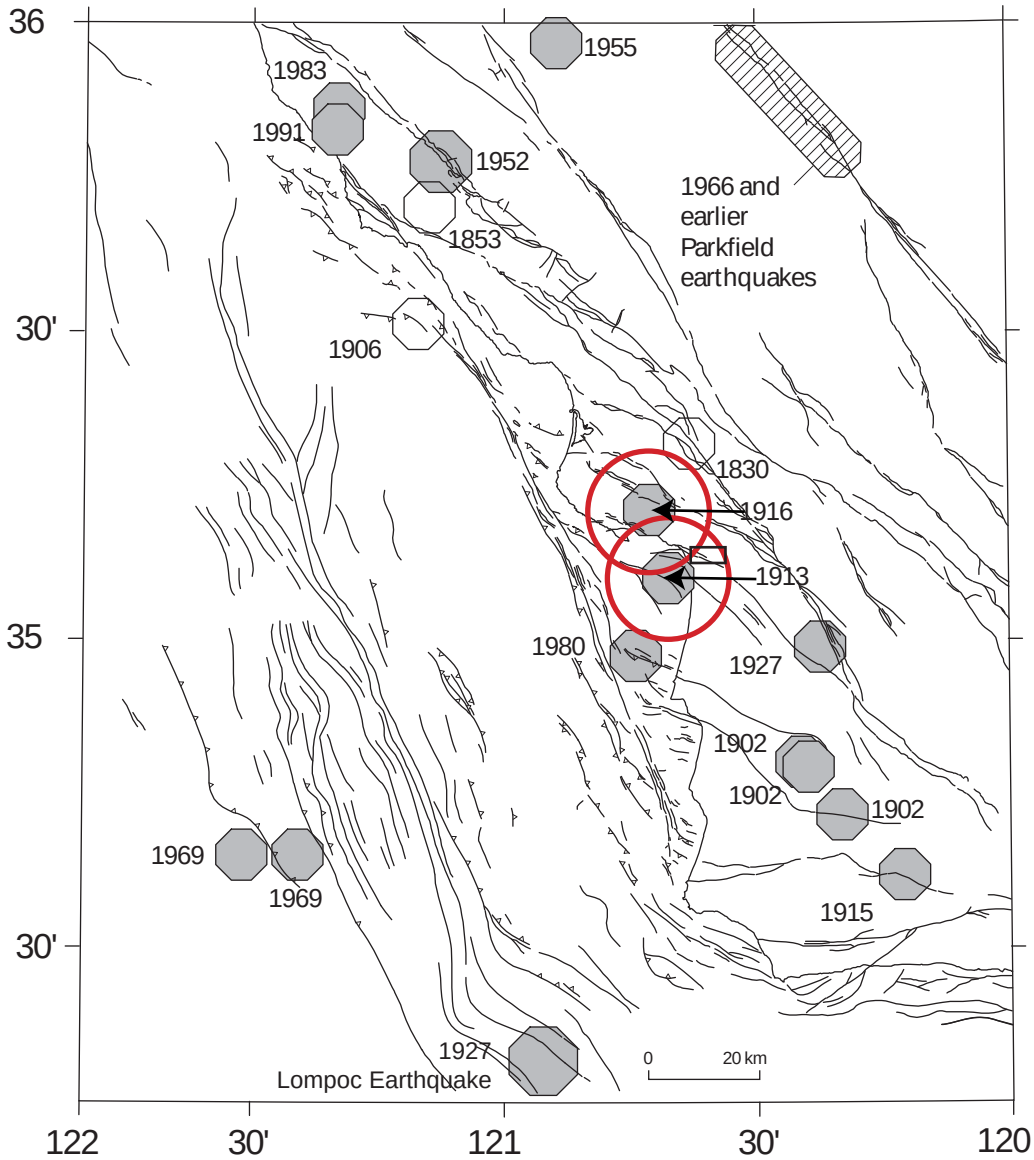

Figure from McLaren and Savage, 2001

EXPLANATION

Event location that is poorly constrained

Event location that is within 20 km and generally within 10 km

10-km radius of uncertainty

Pismo Beach/Arroyo Grande area northeast of the 1913 earthquake

MAGNITUDES

5.0 - 5.9

6.0 - 6.9

7.0 - 7.9

Magnitude 5 and greater pre-1987 historical earthquakes

SHORELINE FAULT ZONE STUDY

Pacific Gas and Electric Company

Figure **4-4**

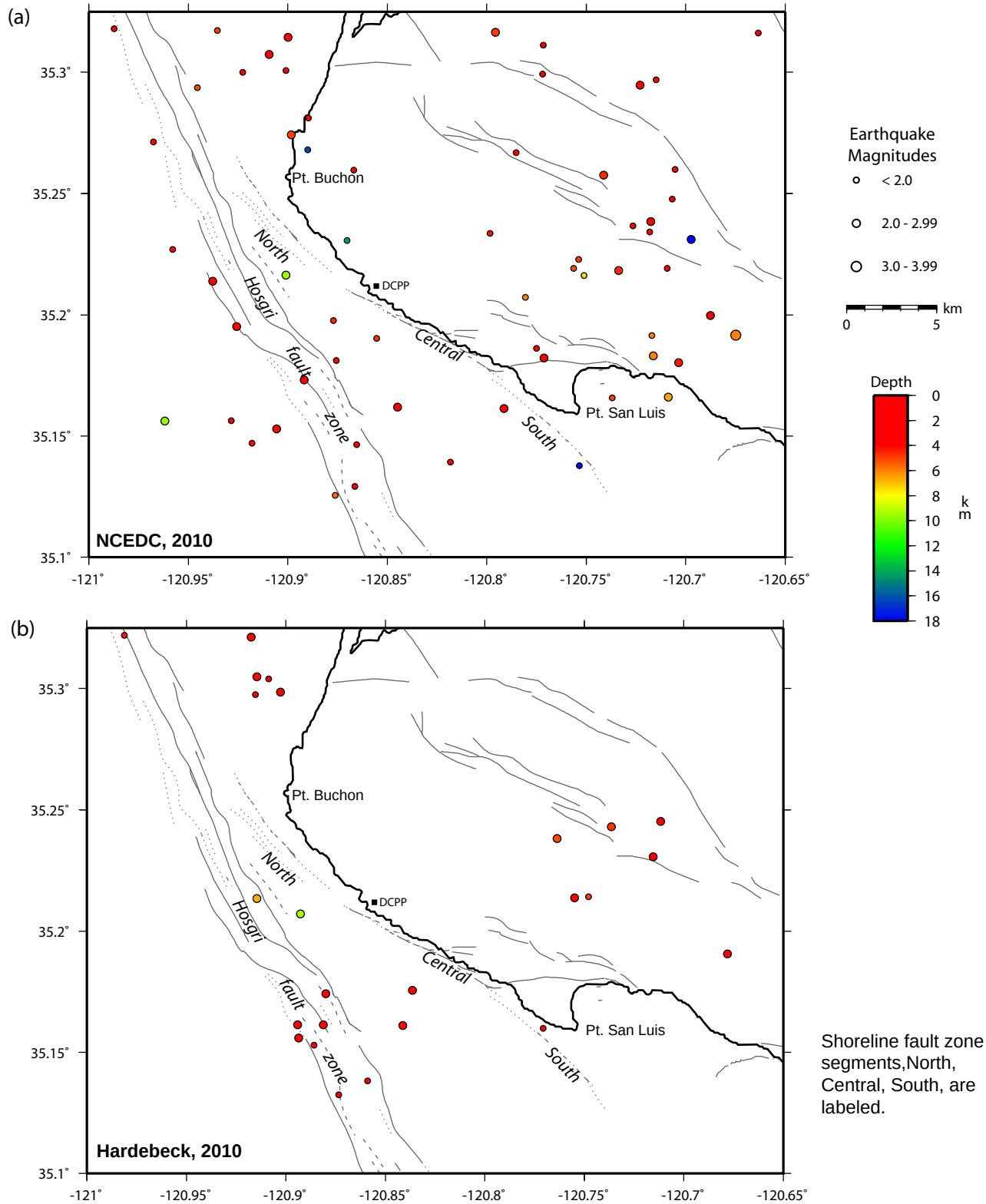

Shoreline fault zone segments,North, Central, South, are labeled.

Comparison of 1970 to 1987 earthquake locations (a) 1-D USGS absolute locations and (b) Hardebeck hypoDD relocations.

SHORELINE FAULT ZONE STUDY

Pacific Gas and Electric Company | Figure **4-5**

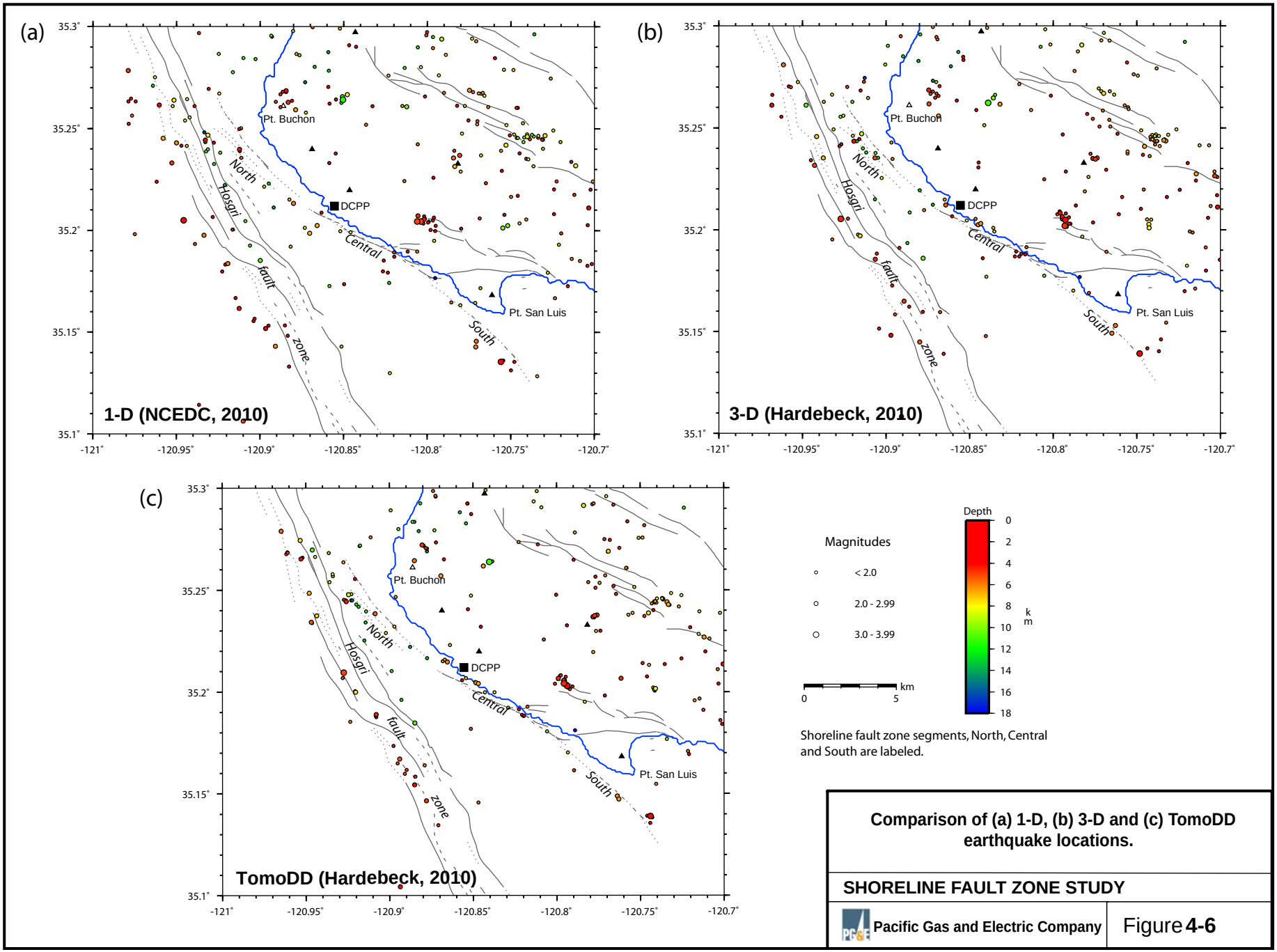

Comparison of (a) 1-D, (b) 3-D and (c) TomoDD earthquake locations.

SHORELINE FAULT ZONE STUDY

Pacific Gas and Electric Company Figure **4-6**

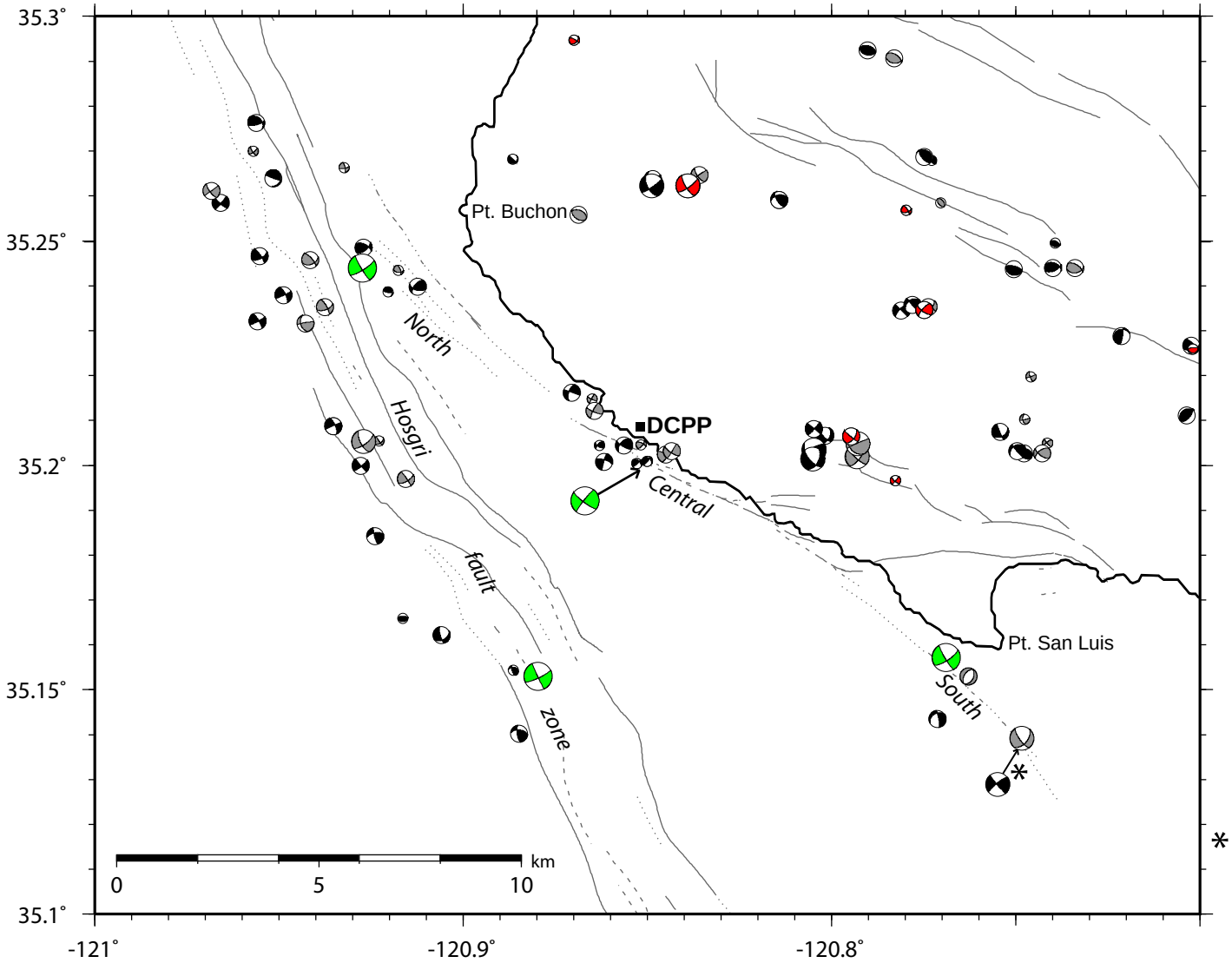

Focal Mechanisms

- <2.0
- 2.0 - 2.9
- 3.0 - 3.9
- Hash Composite Hardebeck, 2010 (HASH; Hardebeck and Shearer, 2002)
- Hash Quality A,B,C Hardebeck, 2010 (HASH; Hardebeck and Shearer, 2002)
- Hash Quality D Hardebeck, 2010 (HASH; Hardebeck and Shearer, 2002)
- FPFIT NCEDC, 2010 (FPFIT; Reasenberg and Oppenheimer, 1985)

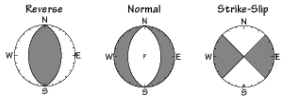

Shoreline fault zone segments, North, Central and South, are labeled.

* HASH & FPFIT focal mechanisms for ML3.5 earthquake on 10 August 2000. Arrow points to approximate FPFIT location.

P- wave first motion focal mechanisms, 1987 through August 2008

SHORELINE FAULT ZONE STUDY

Pacific Gas and Electric Company

Figure **4-7**

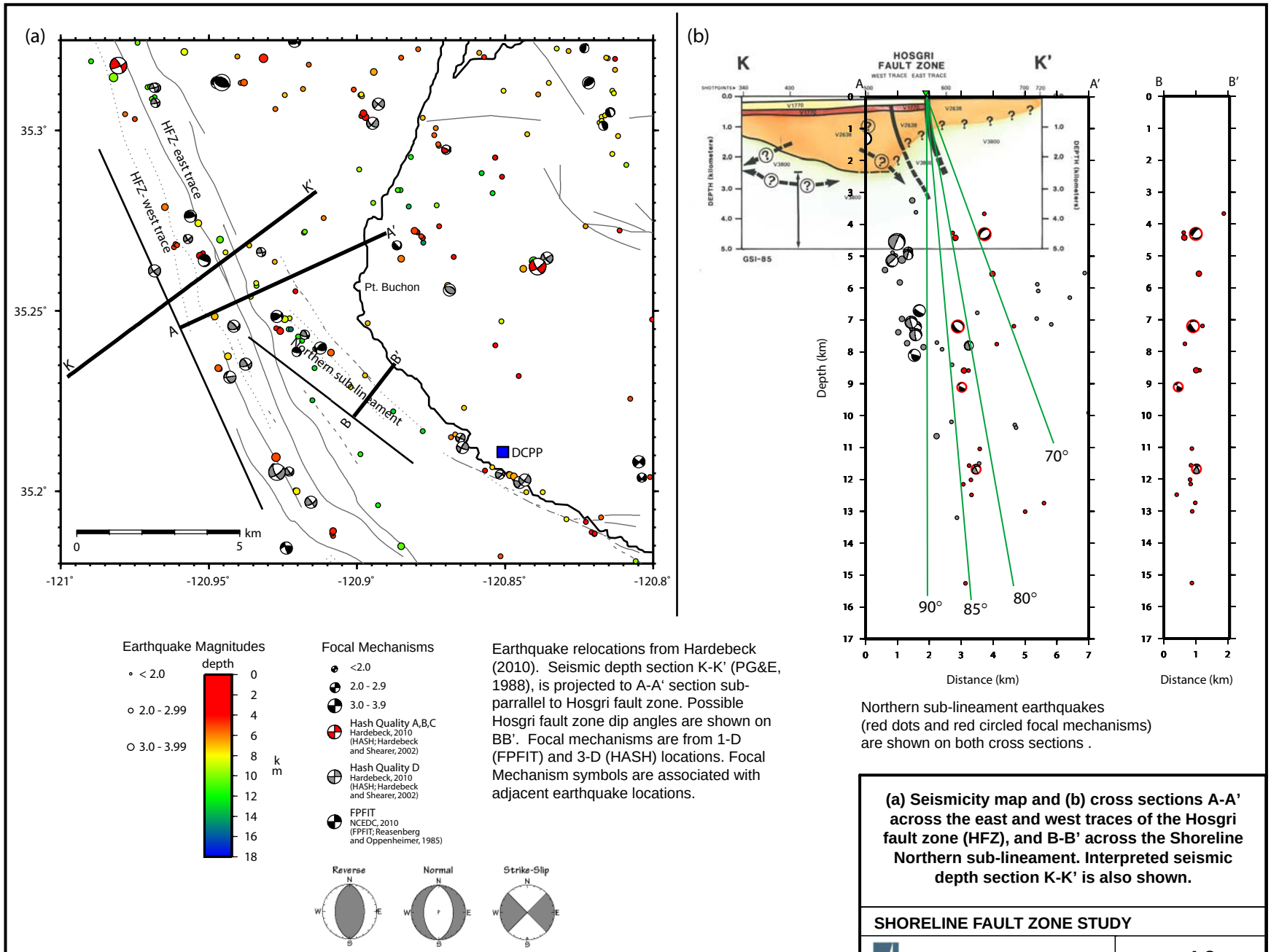

Earthquake relocations from Hardebeck (2010). Seismic depth section K-K' (PG&E, 1988), is projected to A-A' section sub-parrallel to Hosgri fault zone. Possible Hosgri fault zone dip angles are shown on BB'. Focal mechanisms are from 1-D (FPFIT) and 3-D (HASH) locations. Focal Mechanism symbols are associated with adjacent earthquake locations.

Northern sub-lineament earthquakes (red dots and red circled focal mechanisms) are shown on both cross sections .

(a) Seismicity map and (b) cross sections A-A' across the east and west traces of the Hosgri fault zone (HFZ), and B-B' across the Shoreline Northern sub-lineament. Interpreted seismic depth section K-K' is also shown.

SHORELINE FAULT ZONE STUDY

Pacific Gas and Electric Company | Figure **4-8**

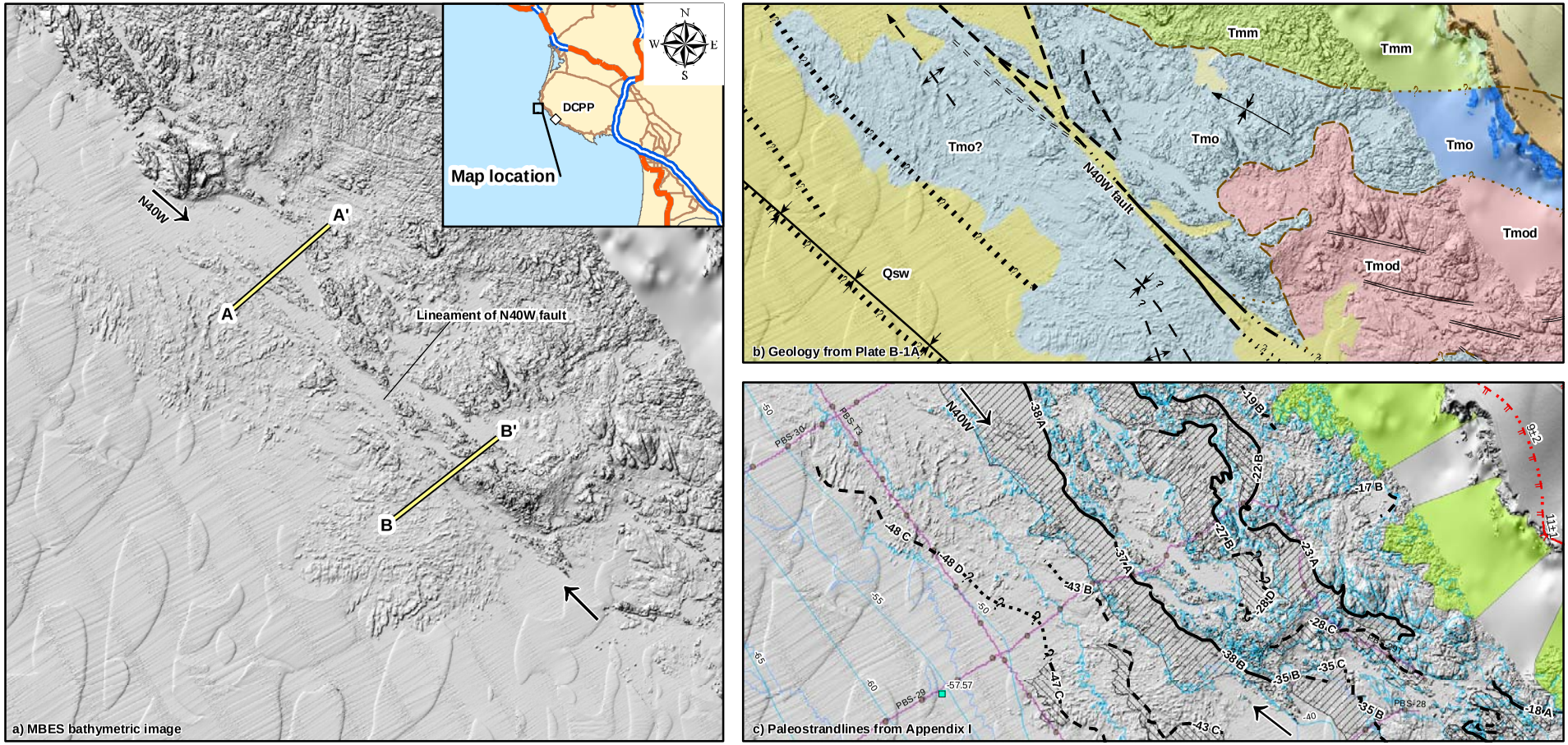

Note: See legend on Plate 1 for geology and Appendix I Plate I-1A for paleostrandlines

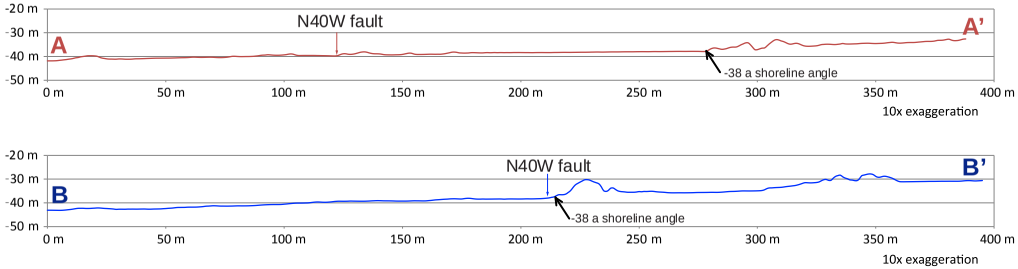

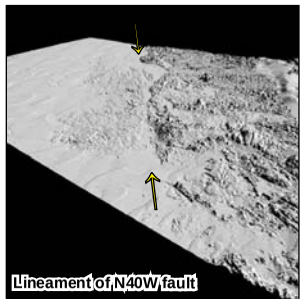

Map scale: 1:12,000
Map projection: NAD 1983, UTM Zone 10 North

0 500 1,000 Feet
0 100 200 300 Meters

Comparison of (a) MBES bathymetric image with (b) the interpreted geology and (c) paleostrandlines across the N40W fault

SHORELINE FAULT ZONE STUDY

Pacific Gas and Electric Company

Figure **4-9**

File path: S:\13800\13838\13838.002\Figures\20101112_Report\Appendix_B\Figure_B1-9_N40W_Lineament.mxd

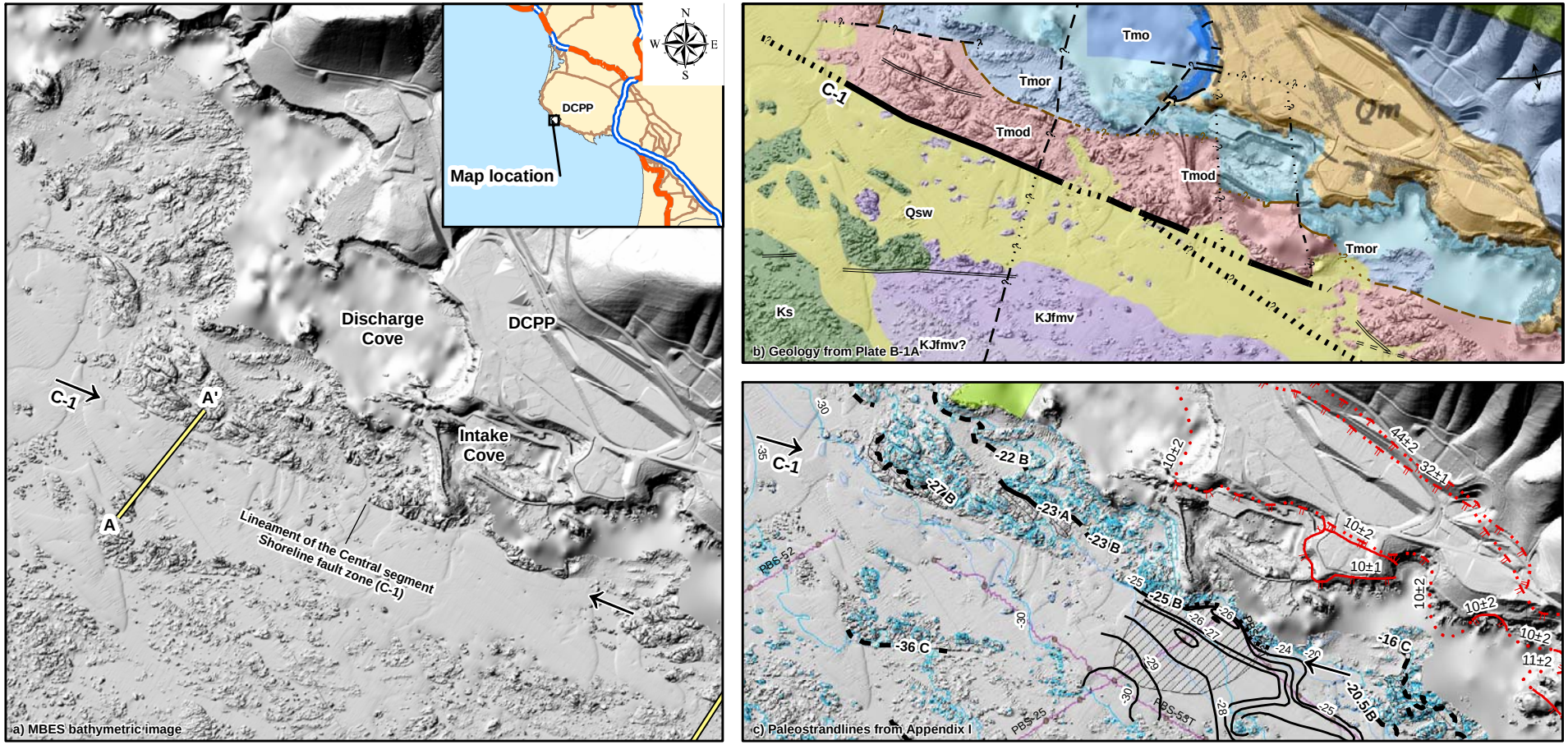

Note: See legend on Plate 1 for geology and Appendix I Plate I-1A for paleostrandlines

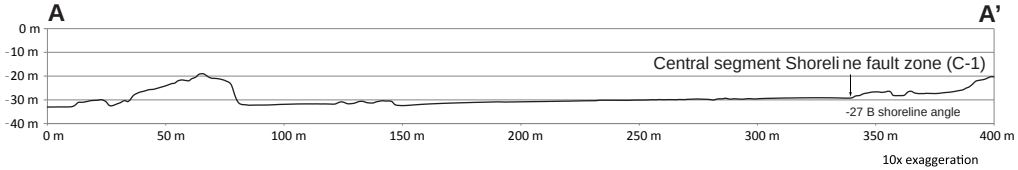

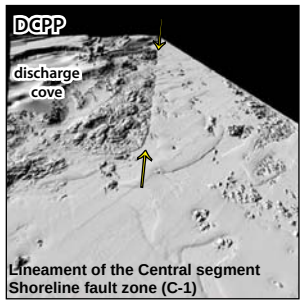

Map scale: 1:12,000
Map projection: NAD 1983, UTM Zone 10 North

0 500 1,000 Feet
0 100 200 300 Meters

Comparison of (a) MBES bathymetry with (b) interpreted geology and (c) paleostrandlines across the Central Segment (C-1) Shoreline fault zone west of DCPP

SHORELINE FAULT ZONE STUDY

Pacific Gas and Electric Company

Figure **4-10**

File path: S:\13800\13838\13838.002\Figures\20101112_Report\Appendix_B\Figure_B-5-5.mxd; Date: [12/20/2010]; User: S. Bozkurt

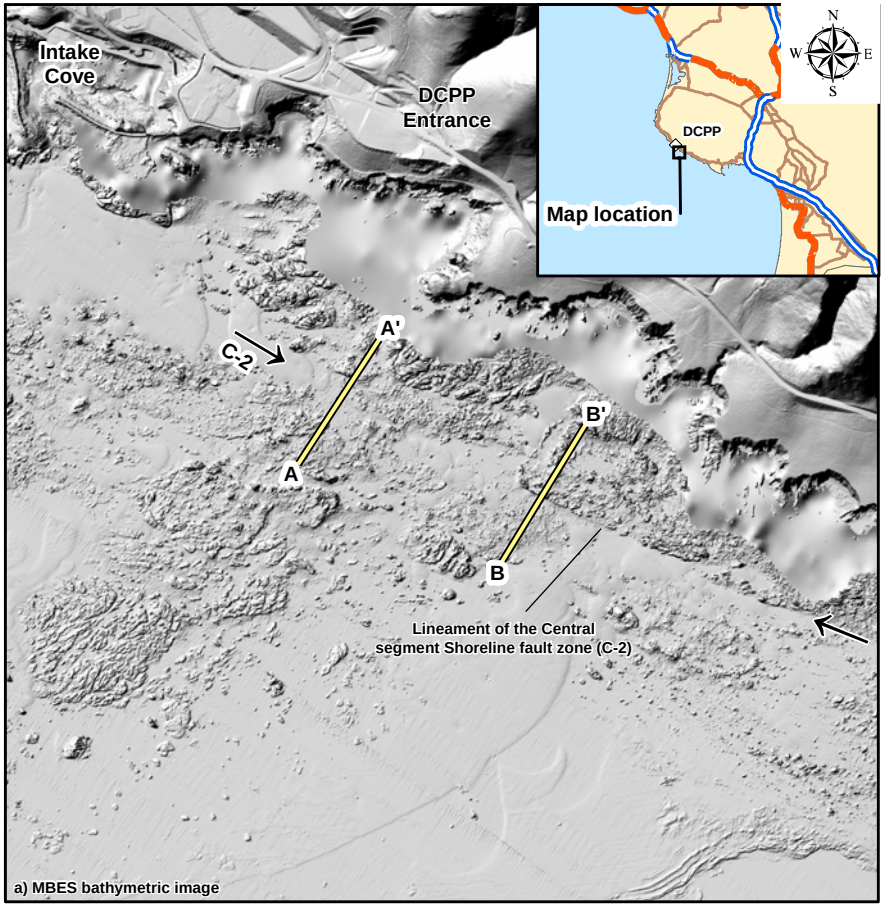

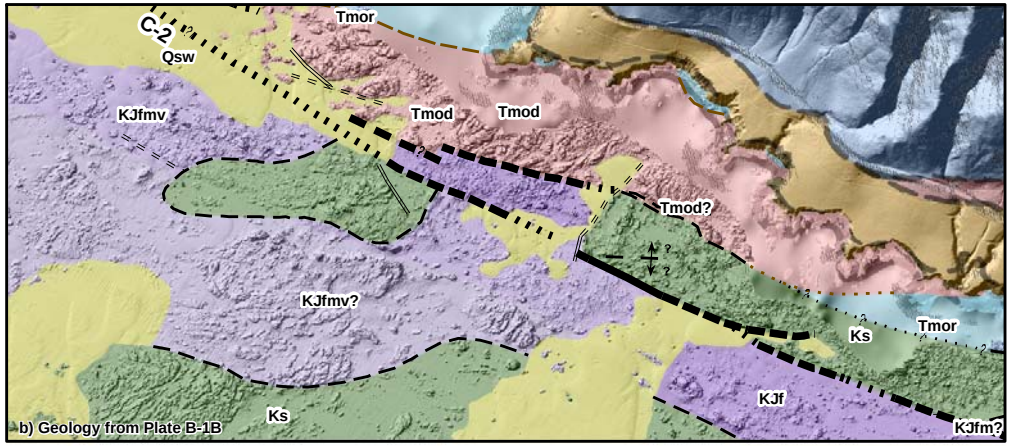

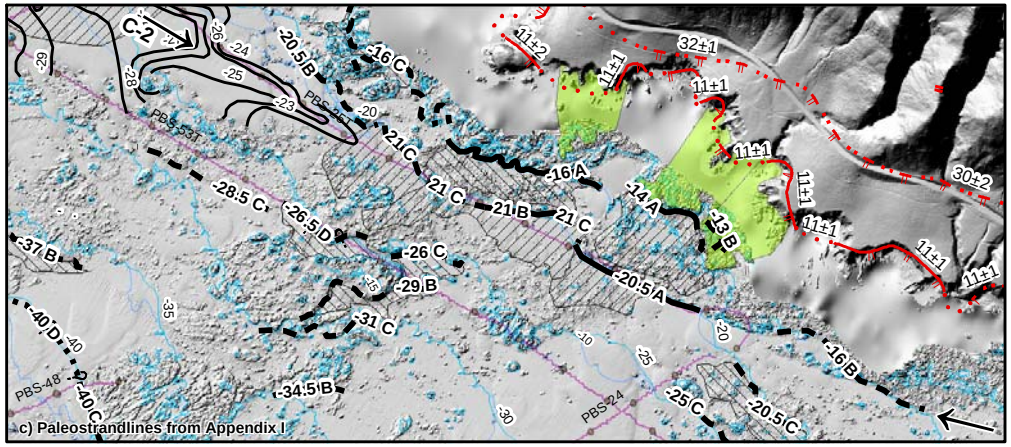

Note: See legend on Plate 1 for geology and Appendix I Plate I-1A for paleostrandlines

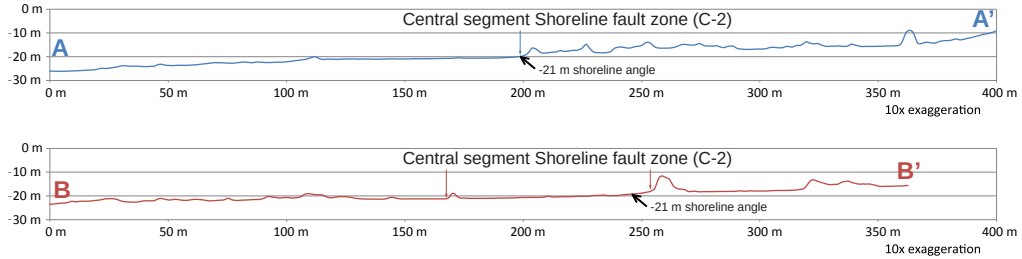

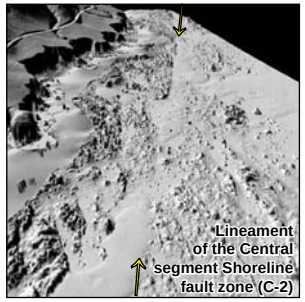

Map scale: 1:12,000
Map projection: NAD 1983, UTM Zone 10 North
0 500 1,000 Feet
0 100 200 300 Meters

Comparison of (a) MBES bathymetry with (b) interpreted geology and (c) paleostrandlines across the Central segment (C-2) Shoreline fault zone southwest of DCPP entrance

SHORELINE FAULT ZONE STUDY

Pacific Gas and Electric Company | Figure **4-11**

File path: S:\13800\13838\13838.002\Figures\20101112_Report\Appendix_B\Figure_B-5-6.mxd; Date: [12/20/2010]; User: S. Bozkurt

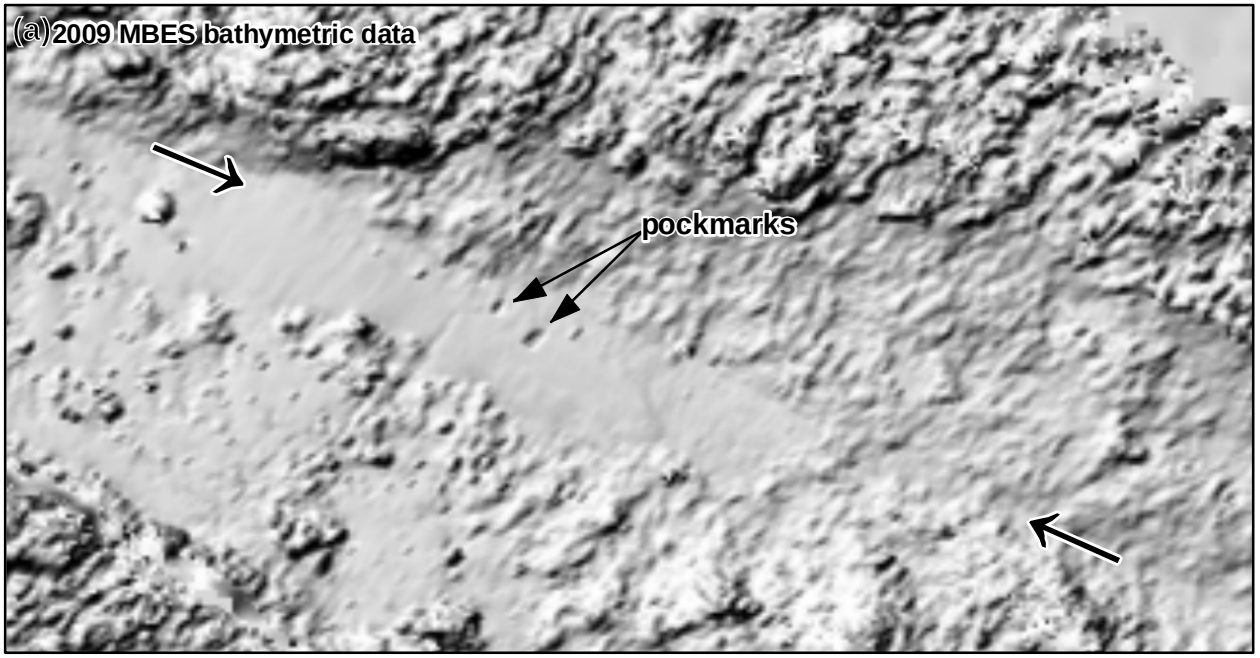

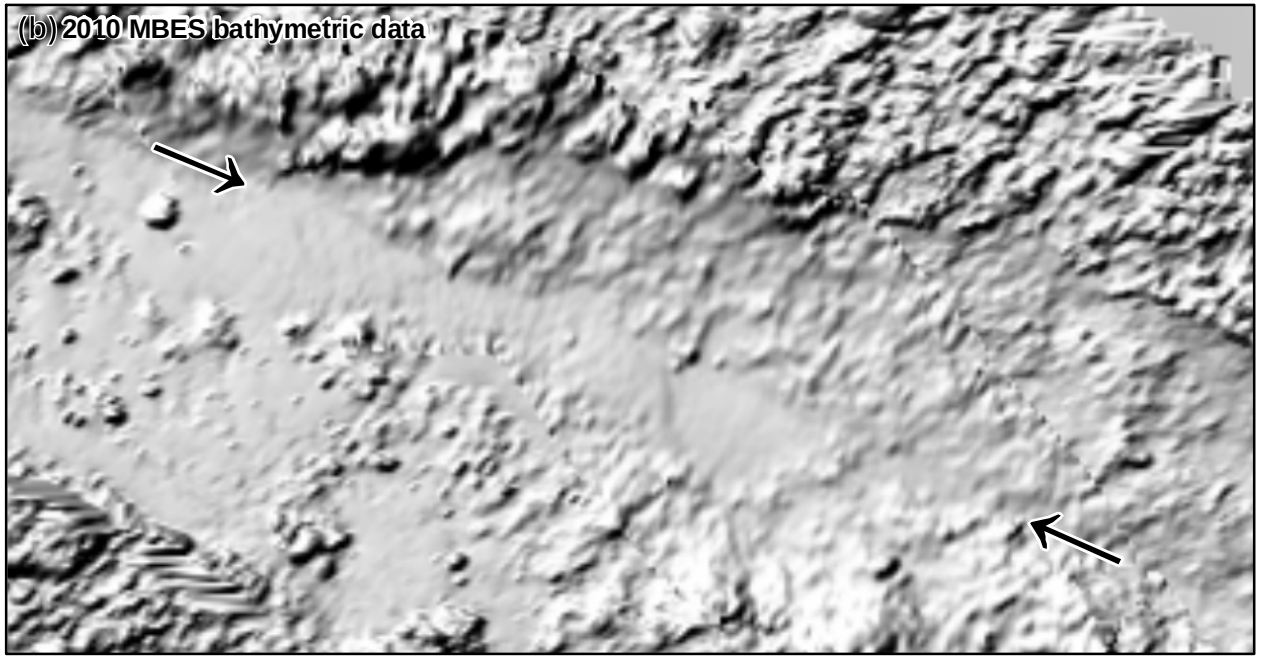

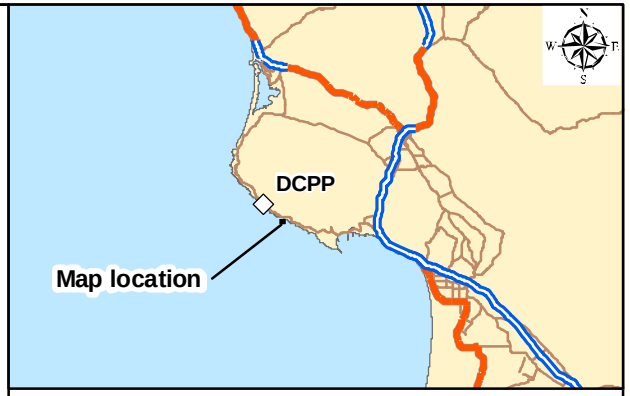

LEGEND

Lineament of Central segment (sub-segment C-2) of the Shoreline fault zone

Notes:
a) The 2009 MBES bathymetric image shows two small pockmarks in the sand sheet that may have been formed by gas or fluid release along the Central segment of the Shoreline fault zone.
b) 2010 MBES bathymetric image of the same area shows the loss of the pockmarks and thinning of the sand sheet, with more bedrock exposed along the fault at the sea floor.

Map scale 1:2,000
Map projection: NAD 1983, UTM Zone 10 North

0 200 400 Feet
0 50 100 Meters

Migration of sand sheet along the Central segment (C-2) of the Shoreline fault zone between (a) the 2009 and (b) 2010 MBES surveys northwest of Olson Hill

SHORELINE FAULT ZONE STUDY

Pacific Gas and Electric Company

Figure **4-12**

File path: S:\13800\13838\13838.002\Figures\20101112_Report\Appendix_B\Figure_B-3-5.mxd; Date: [12/22/2010]; User: Serkan Bozkurt, AMEC Geomatrix, Inc.

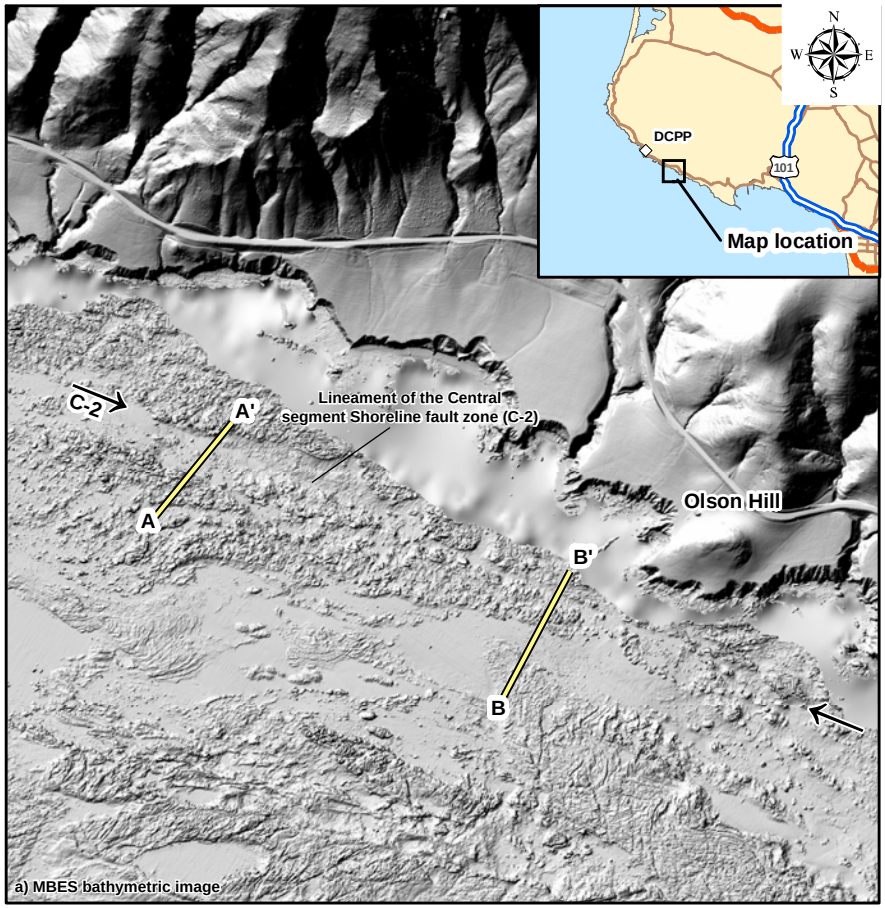

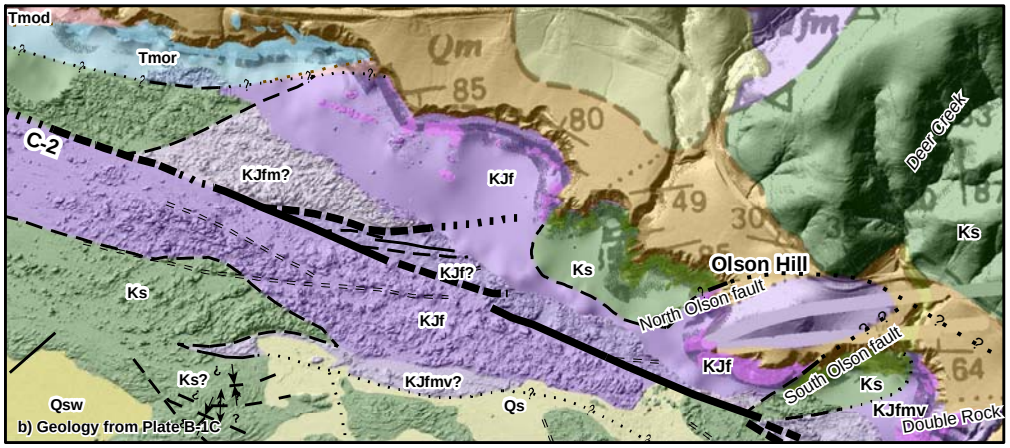

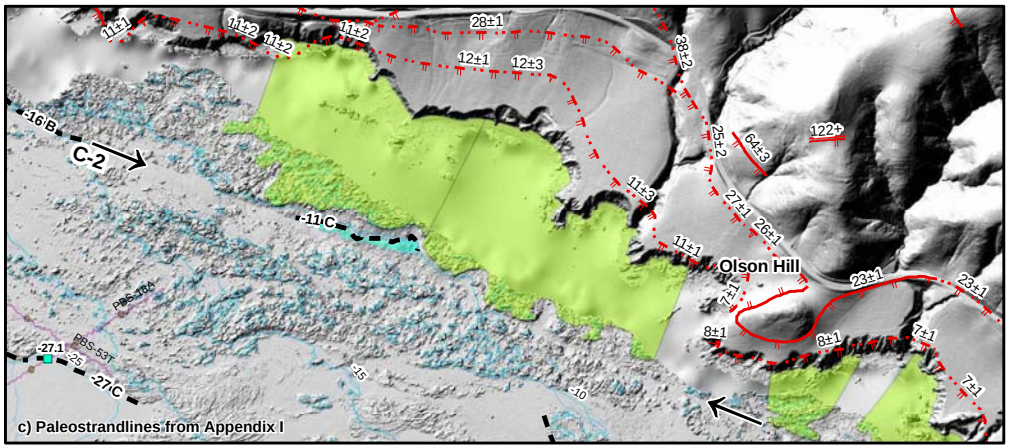

Note: See legend on Plate 1 for geology and Appendix I Plate I-1A for paleostrandlines

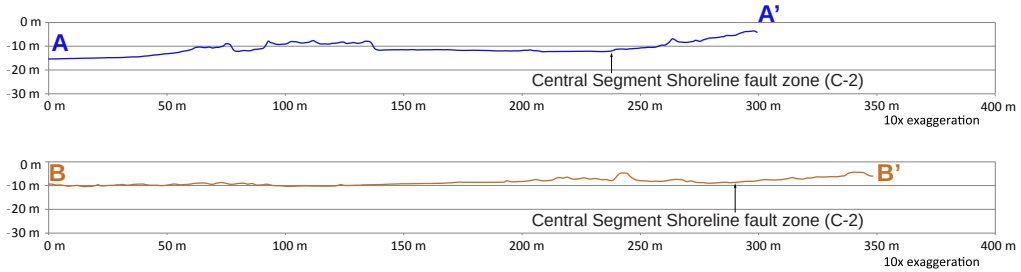

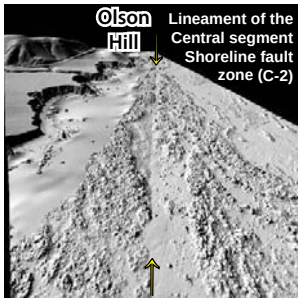

Map scale: 1:12,000
Map projection: NAD 1983, UTM Zone 10 North

0 500 1,000 Feet
0 100 200 300 Meters

Comparison of (a) MBES bathymetry with (b) interpreted geology and (c) paleostrandlines across the Central segment (C-2) Shoreline fault zone west of Olson Hill

SHORELINE FAULT ZONE STUDY

Pacific Gas and Electric Company | Figure **4-13**

File path: S:\13800\138380\138380.002\Figures\20101112_Report\Appendix_B\Figure_B-5-8.mxd; Date: [12/20/2010]; User: S. Bozkurt

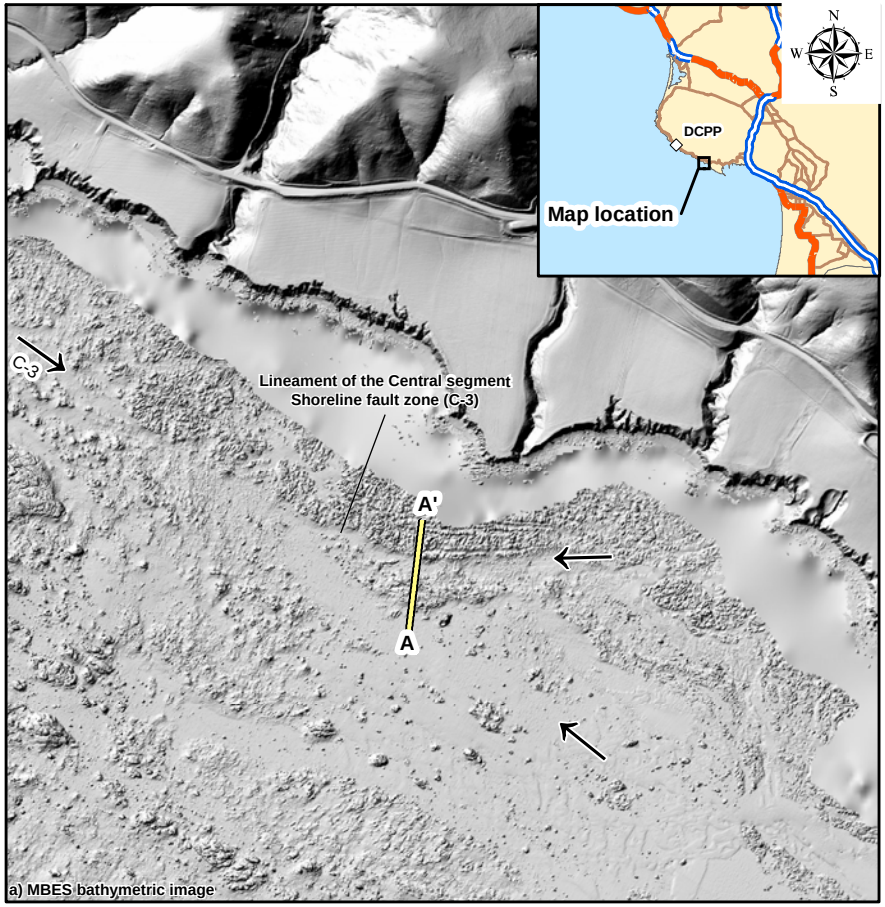

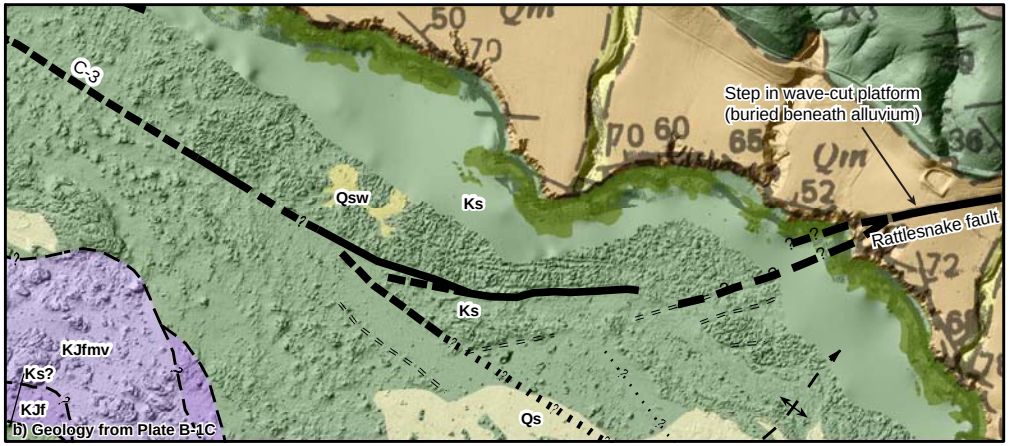

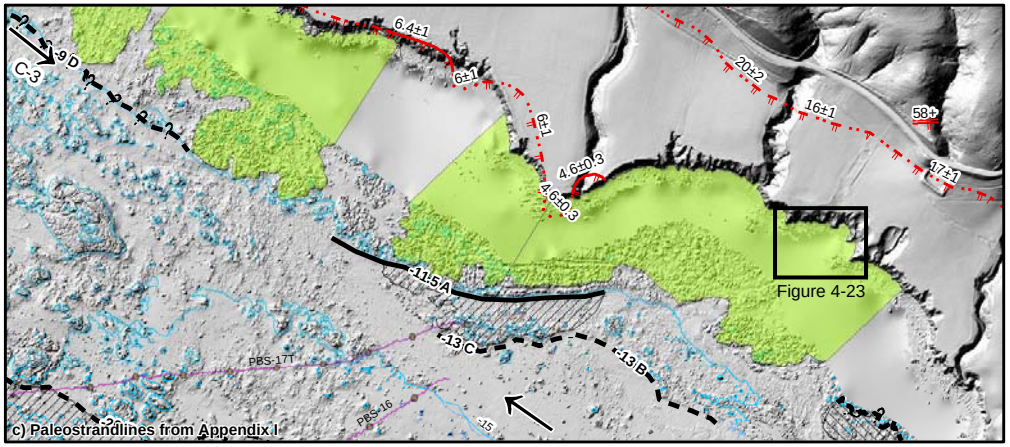

Note: See legend on Plate 1 for geology and Appendix I Plate I-1A for paleostrandlines

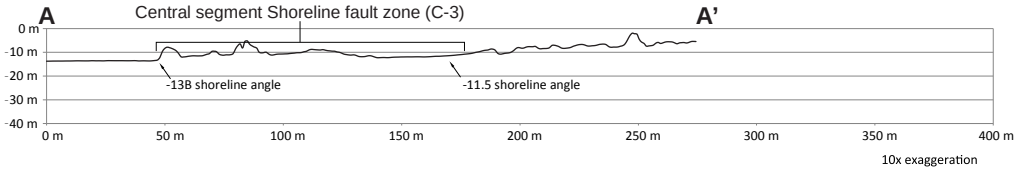

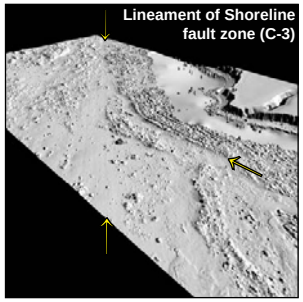

Map scale: 1:12,000
Map projection: NAD 1983, UTM Zone 10 North

0 500 1,000 Feet
0 100 200 300 Meters

Comparison of (a) MBES bathymetry with (b) interpreted geology and (c) paleostrandlines across the Central segment (C-3) of the Shoreline fault zone west of Rattlesnake Creek

SHORELINE FAULT ZONE STUDY

Pacific Gas and Electric Company | Figure **4-14**

File path: S:\13800\138388\138388.002\Figures\20101112_Report\Appendix_B\Figure_B-5-9.mxd; Date: [12/20/2010]; User: S. Bozkurt

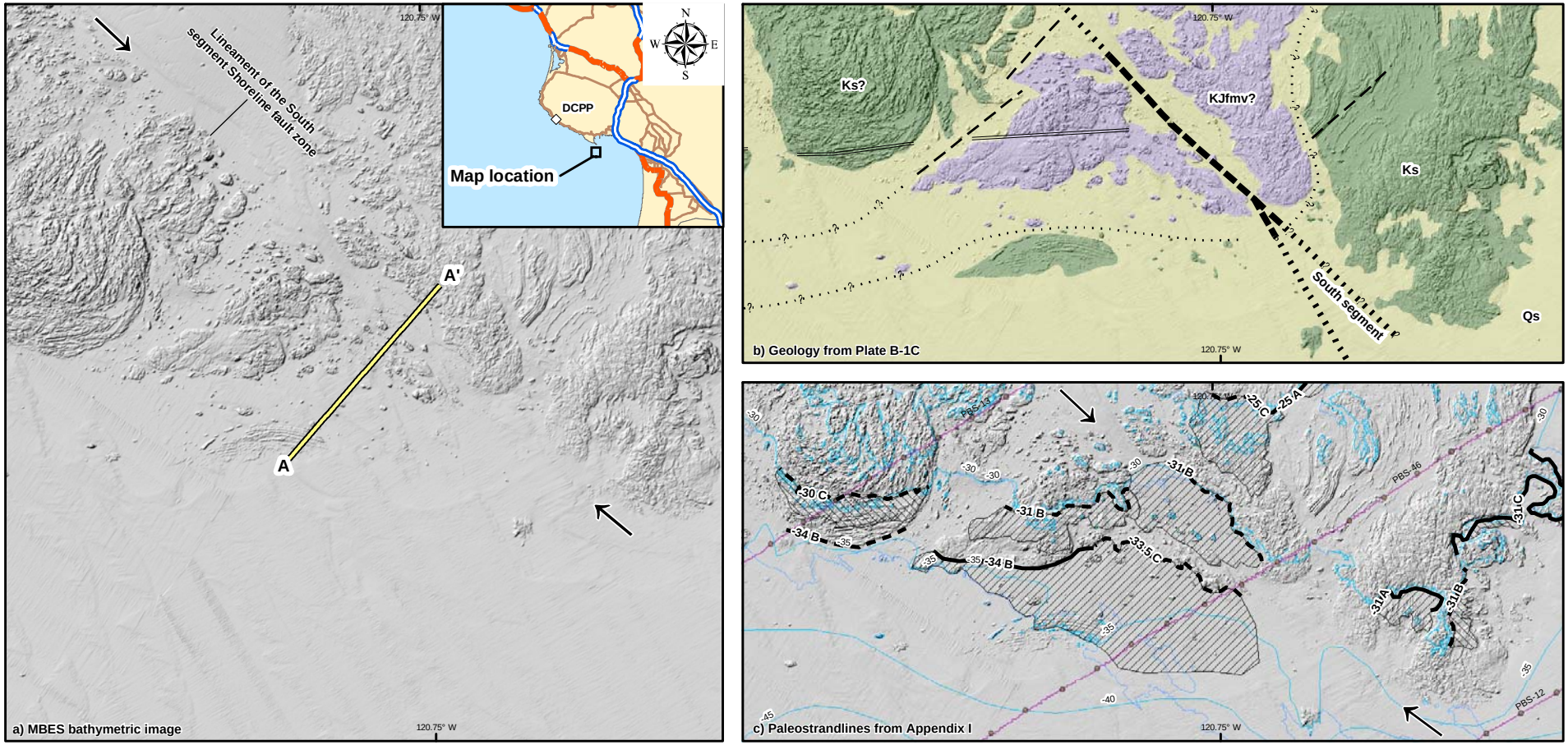

Note: See legend on Plate 1 for geology and Appendix I Plate I-1A for paleostrandlines

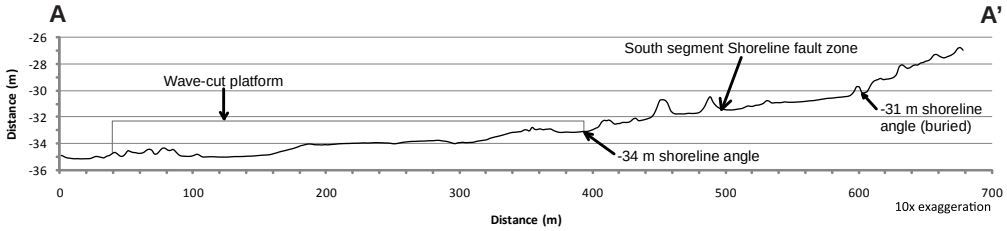

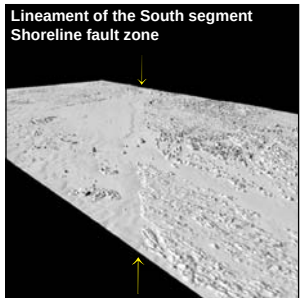

Map scale: 1:12,000
Map projection: NAD 1983, UTM Zone 10 North
0 500 1,000 Feet
0 100 200 300 Meters

Comparison of (a) MBES bathymetry with (b) interpreted geology and (c) paleostrandlines across the South segment of the Shoreline fault zone south of Point San Luis

SHORELINE FAULT ZONE STUDY

Pacific Gas and Electric Company | Figure **4-15**

File path: S:\13800\13838\13838.002\Figures\20101112_Report\Appendix_B\Figure_B-5-10.mxd; Date: [12/21/2010]; User: S. Bozkurt

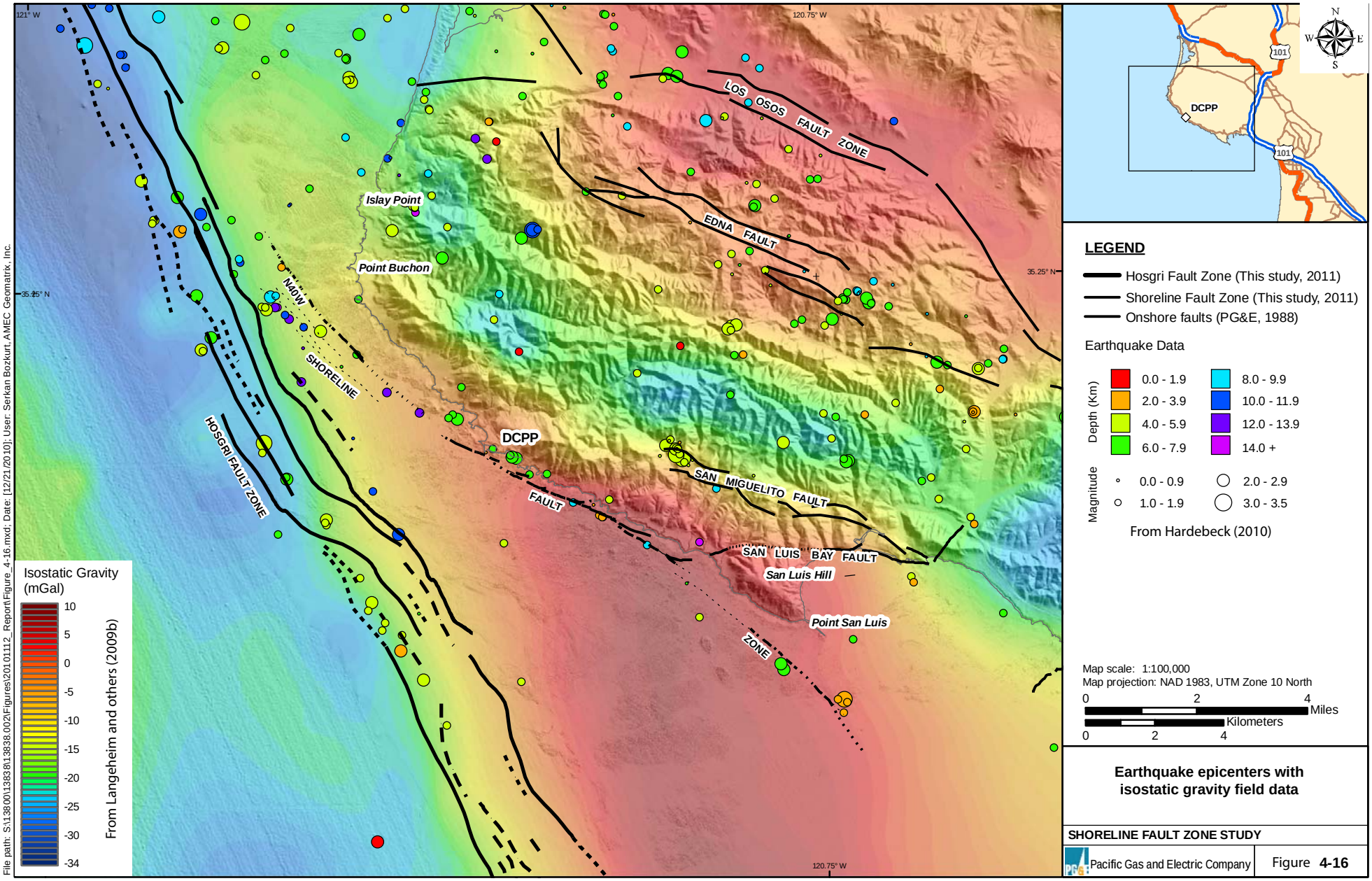
121° W
120.75° W
35.25° N
LOS OSOS FAULT ZONE
EDNA FAULT
Islay Point
Point Buchon
N40W
SHORELINE
HOSGRI FAULT ZONE
DCPP
SAN MIGUELITO FAULT
FAULT
SAN LUIS BAY FAULT
San Luis Hill
Point San Luis
ZONE
Isostatic Gravity (mGal)
10
5
0
-5
-10
-15
-20
-25
-30
-34
From Langeheim and others (2009b)
DCPP
101
N
S
E
W
LEGEND
Hosgri Fault Zone (This study, 2011)
Shoreline Fault Zone (This study, 2011)
Onshore faults (PG&E, 1988)
Earthquake Data
Depth (Km)
0.0 - 1.9
2.0 - 3.9
4.0 - 5.9
6.0 - 7.9
8.0 - 9.9
10.0 - 11.9
12.0 - 13.9
14.0 +
Magnitude
0.0 - 0.9
1.0 - 1.9
2.0 - 2.9
3.0 - 3.5
From Hardebeck (2010)
Map scale: 1:100,000
Map projection: NAD 1983, UTM Zone 10 North
0
2
4
Miles
Kilometers
0
2
4
Earthquake epicenters with isostatic gravity field data
SHORELINE FAULT ZONE STUDY
Pacific Gas and Electric Company
Figure 4-16
File path: S:\138000\138838\138838.002\Figures\20101112_Report\Figure_4-16.mxd; Date: [12/21/2010]; User: Serkan Bozkurt, AMEC Geomatrix, Inc.

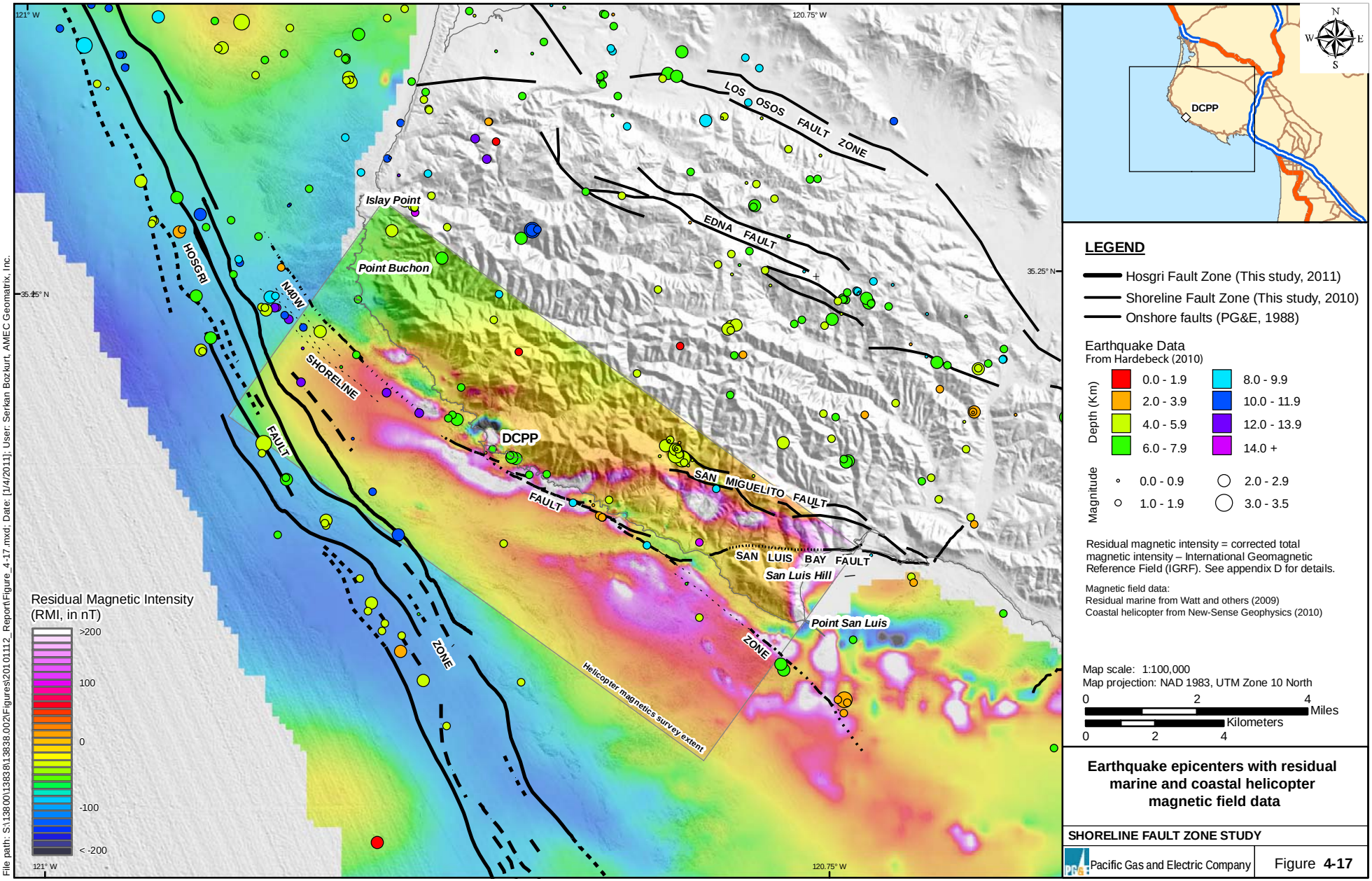

Earthquake epicenters with residual marine and coastal helicopter magnetic field data

SHORELINE FAULT ZONE STUDY

Pacific Gas and Electric Company

Figure **4-17**

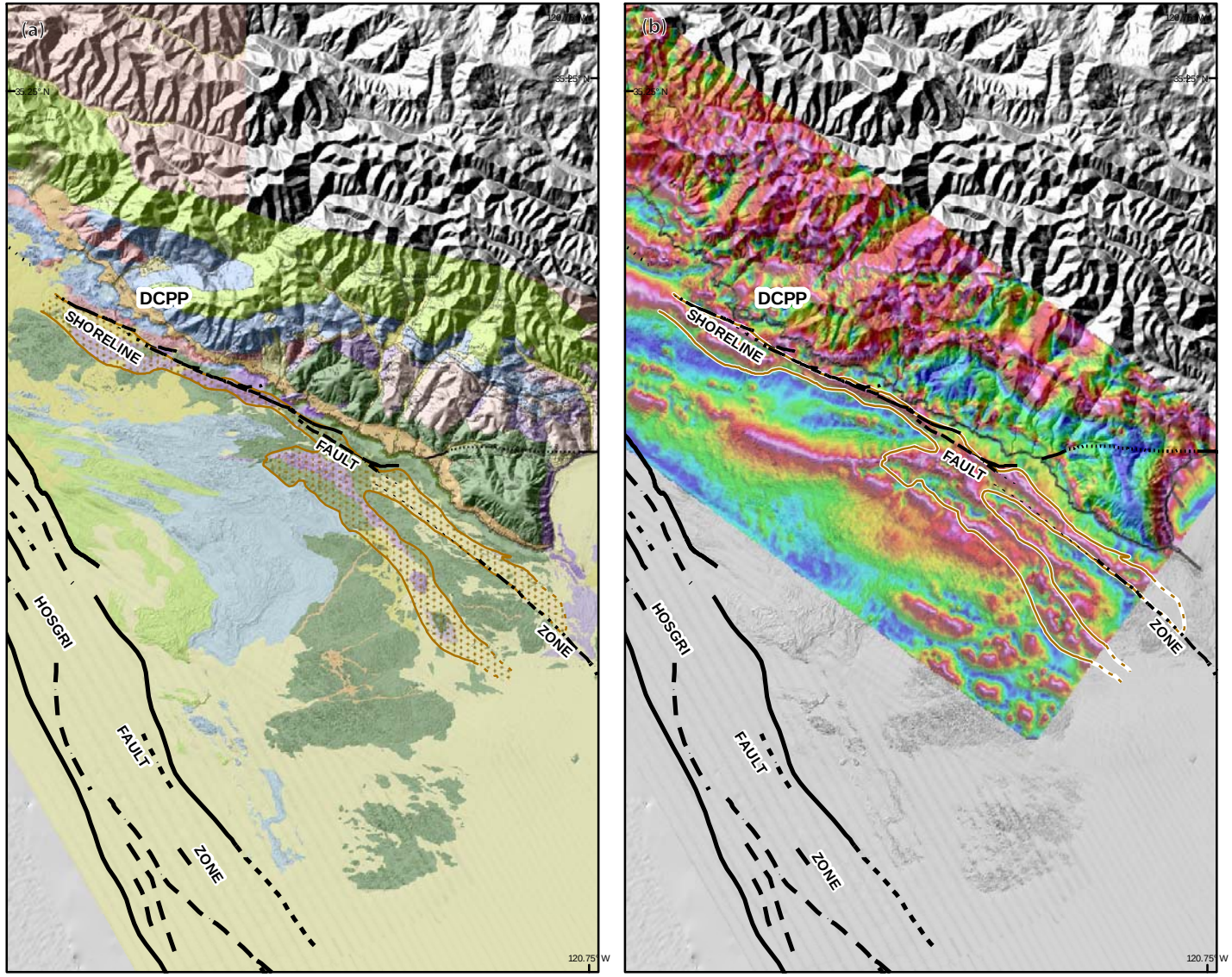

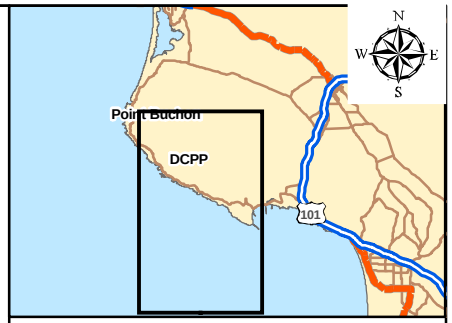

LEGEND

Area of Franciscan mélange interpreted from geology at sea floor or beneath thin sand sheet

Mélange bounding line from geologic map on magnetic image

Faults (This study, 2011)

2010 Helicopter Magnetic Survey

45
21
-1
-21
-39
-55
-67
-78

Tilt angle of RTP is shown in degrees

See Appendix D for discussion of magnetic data

Notes:
See Plate 1 for geology legend.
The Central and Southern segments of the Shoreline fault zone lie within the Franciscan mélange and generally follow magnetic highs.

Map scale: 1:90,000
Map projection: NAD 1983, UTM Zone 10 North

0 1 2 Miles
0 2 4 Kilometers

Generalized area of (a) Franciscan mélange offshore compared to (b) magnetic-field anomalies

SHORELINE FAULT ZONE STUDY

Pacific Gas and Electric Company

Figure **4-18**

File path: S:\13800\13838\13838.002\Figures\20101112_Report\Appendix_B\Figure_B-4-4.mxd; Date: [12/20/2010]; User: Serkan Bozkurt, AMEC Geomatrix, Inc.

(a) Comap Line CM-23

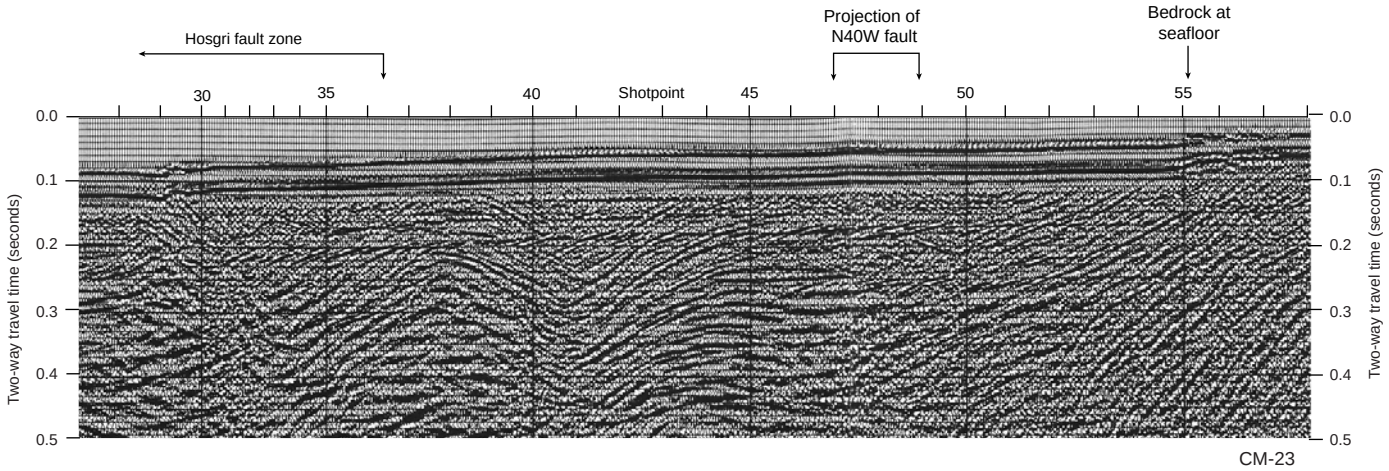

(b) Comap Line CM-21

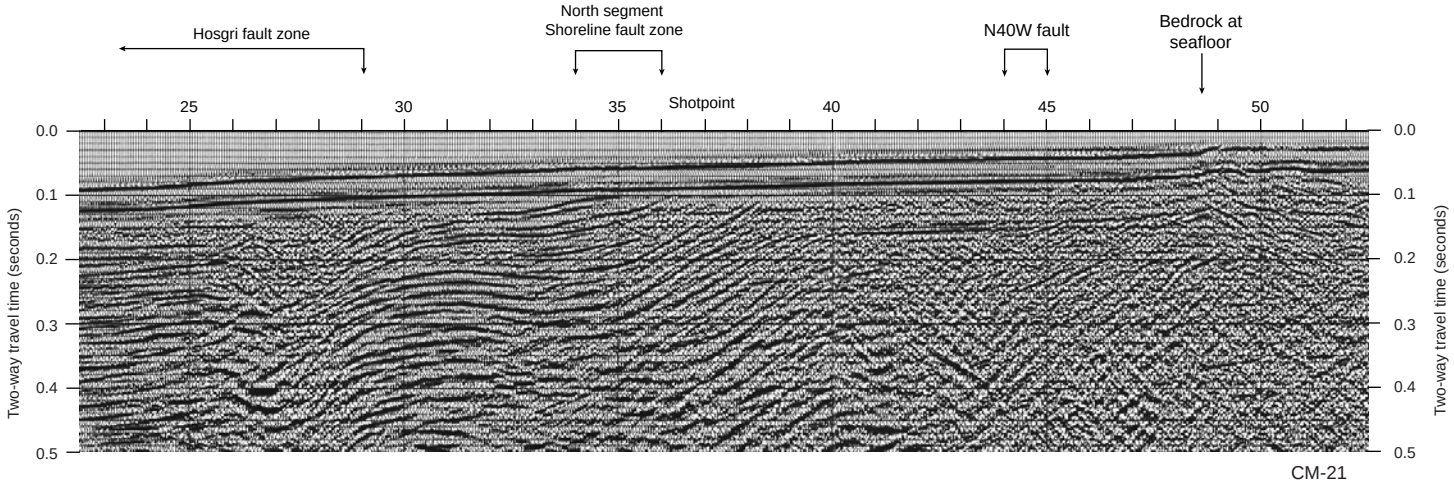

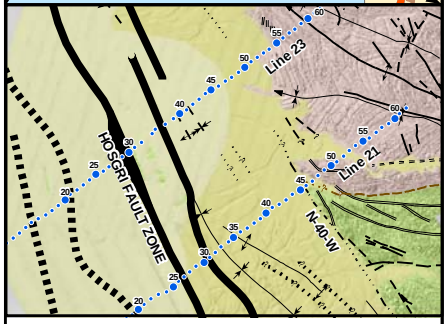

Note: Comap profiles (upper 0.5 seconds) (PG&E, 1988). CM-23 images the eatern part of the Hosgri fault zone but not the N40W fault. CM-21 images the eastern part of the Hosgri fault zone and the N40W fault. No fault is detected in the seismic-reflection profile across the northern Shoreline seismicity lineament.

Comap seismic-reflection profiles (a) CM-23 and (b) CM-21 across the Hosgri fault zone, North segment of the Shoreline fault zone and the N40W fault.

SHORELINE FAULT ZONE STUDY

Pacific Gas and Electric Company | Figure **4-19**

File path: S:\13800\13838\13838.002\Figures\20101112_Report\Appendix_B\Figure_B-5-3.ai; Date: [12/21/2010]; User: S. Bozkurt

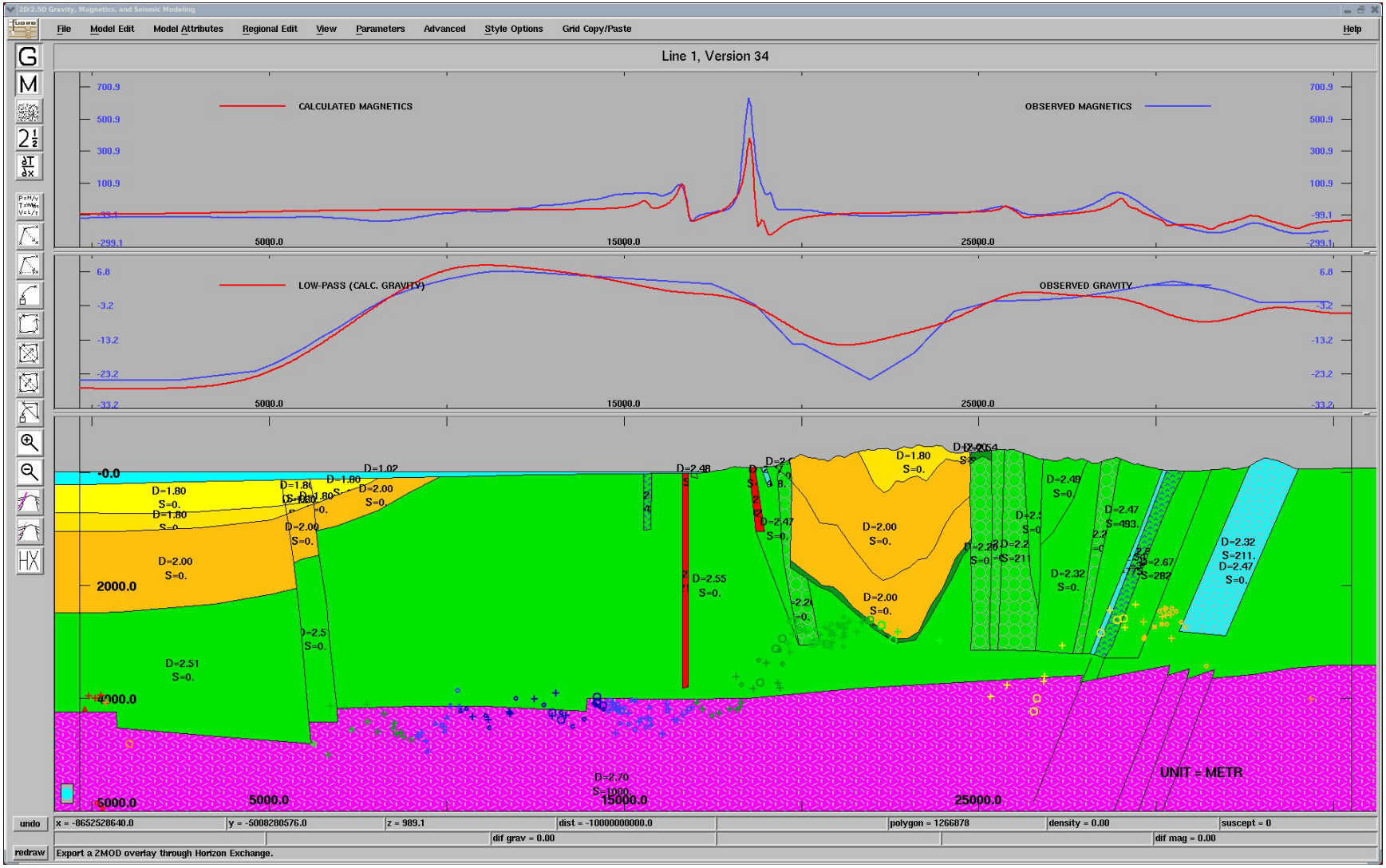

Cross Section of geology, magnetic inversion and gravity through Olson Hill

SHORELINE FAULT ZONE STUDY

Pacific Gas and Electric Company

Figure **4-20**

File path: S:\13800\13838\13838.002\Figures\20101112_Report\Figure_4-20.ai; Date: [12/21/2010]; User: S. Bozkurt

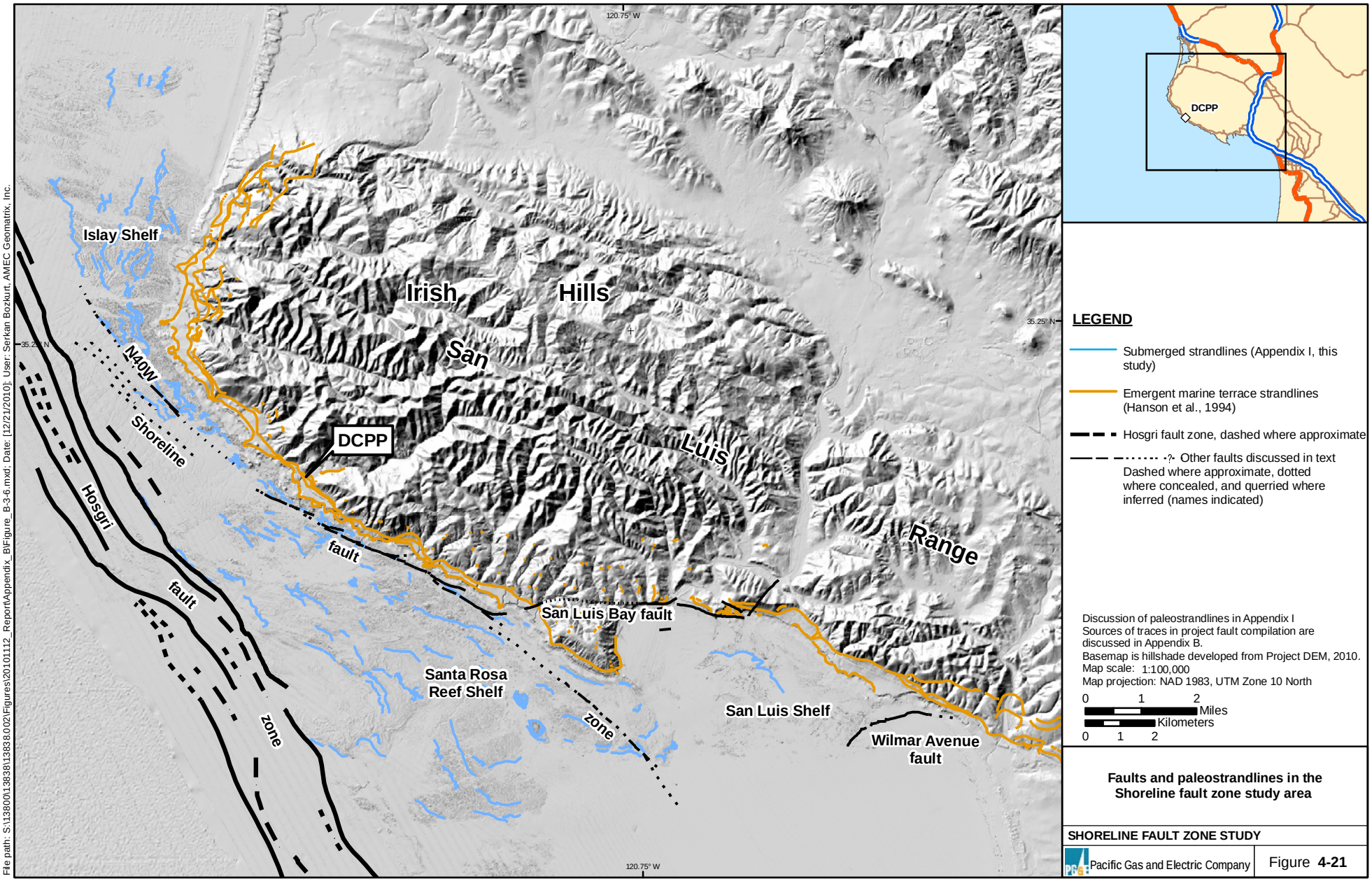
Islay Shelf
Irish
Hills
San
Luis
Range
DCPP
N40W
Shoreline
Hosgri
fault
fault
zone
fault
San Luis Bay fault
Santa Rosa
Reef Shelf
zone
San Luis Shelf
Wilmar Avenue
fault
120.75° W
35.25° N
DCPP
LEGEND
Submerged strandlines (Appendix I, this study)
Emergent marine terrace strandlines (Hanson et al., 1994)
Hosgri fault zone, dashed where approximate
Other faults discussed in text Dashed where approximate, dotted where concealed, and querried where inferred (names indicated)
Discussion of paleostrandlines in Appendix I
Sources of traces in project fault compilation are discussed in Appendix B.
Basemap is hillshade developed from Project DEM, 2010.
Map scale: 1:100,000
Map projection: NAD 1983, UTM Zone 10 North
0 1 2
Miles
Kilometers
0 1 2
Faults and paleostrandlines in the Shoreline fault zone study area
SHORELINE FAULT ZONE STUDY
Pacific Gas and Electric Company
Figure 4-21
File path: S:\13800\13838\13838.002\Figures\20101112_Report\Appendix_B\Figure_B-3-6.mxd; Date: [12/21/2010]; User: Serkan Bozkurt, AMEC Geomatrix, Inc.

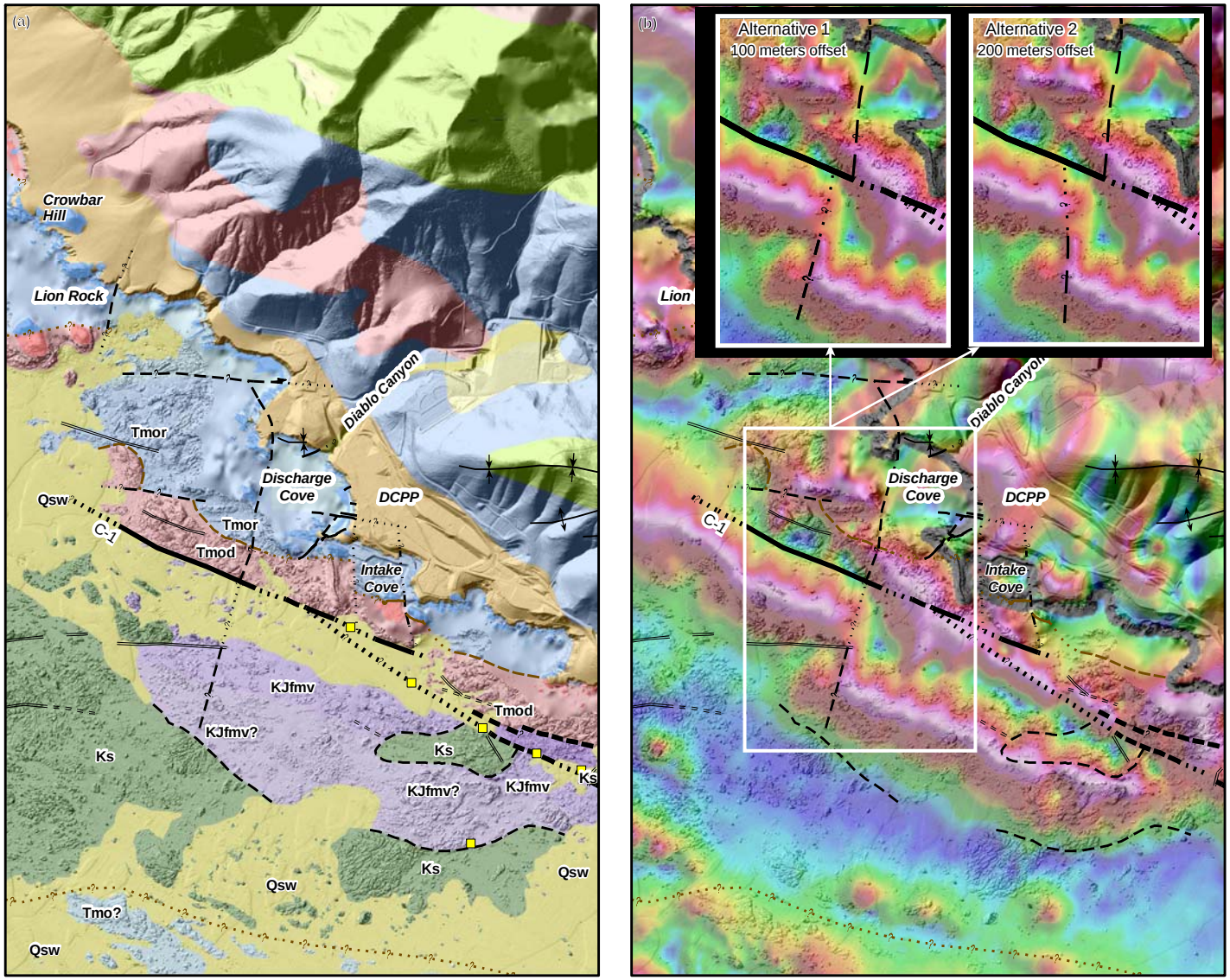

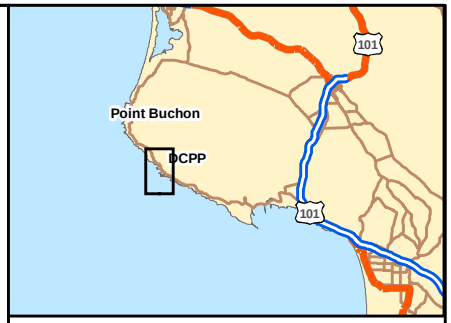

LEGEND

45
21
-1
-21
-39
-55
-67
-78

2010 Helicopter Magnetic Survey Enhancement

Tilt angle of RTP is shown in degrees

See Appendix D for discussion of magnetic data

Notes:
The onshore right-lateral north-south fault north of Discharge Cove aligns with a north-south offset of two northwest-trending magnetic highs. The magnetic anomalies are interpreted to be offset by the same north-south fault. The Shoreline fault does not appear to displace the north-south fault laterally within the limits of resolution (estimated to be about 100 meters per "Alternative 1" but clearly less than 200 meters per "Alternative 2").

See Plate 1 for geology legend.

Map scale: 1:20,000
Map projection: NAD 1983, UTM Zone 10 North

0 1,000 2,000 Feet

0 500 1,000 Meters

Comparison of (a) the geology with (b) the magnetic-field anomalies in the DCPP area

SHORELINE FAULT ZONE STUDY

Pacific Gas and Electric Company

Figure **4-22**

File path: S:\138001\3838\13838.002\Figures\20101112_Report\Appendix_B\Figure_B-5-1.mxd; Date: [12/20/2010]; User: S. Bozkurt

File path: S:\13800\13838\13838.002\Figures\20101112_Report\Appendix_B\Figure_B-5-10.ai; Date: [12/21/2010]; User: Serkan Bozkurt, AMEC Geomatrix, Inc.

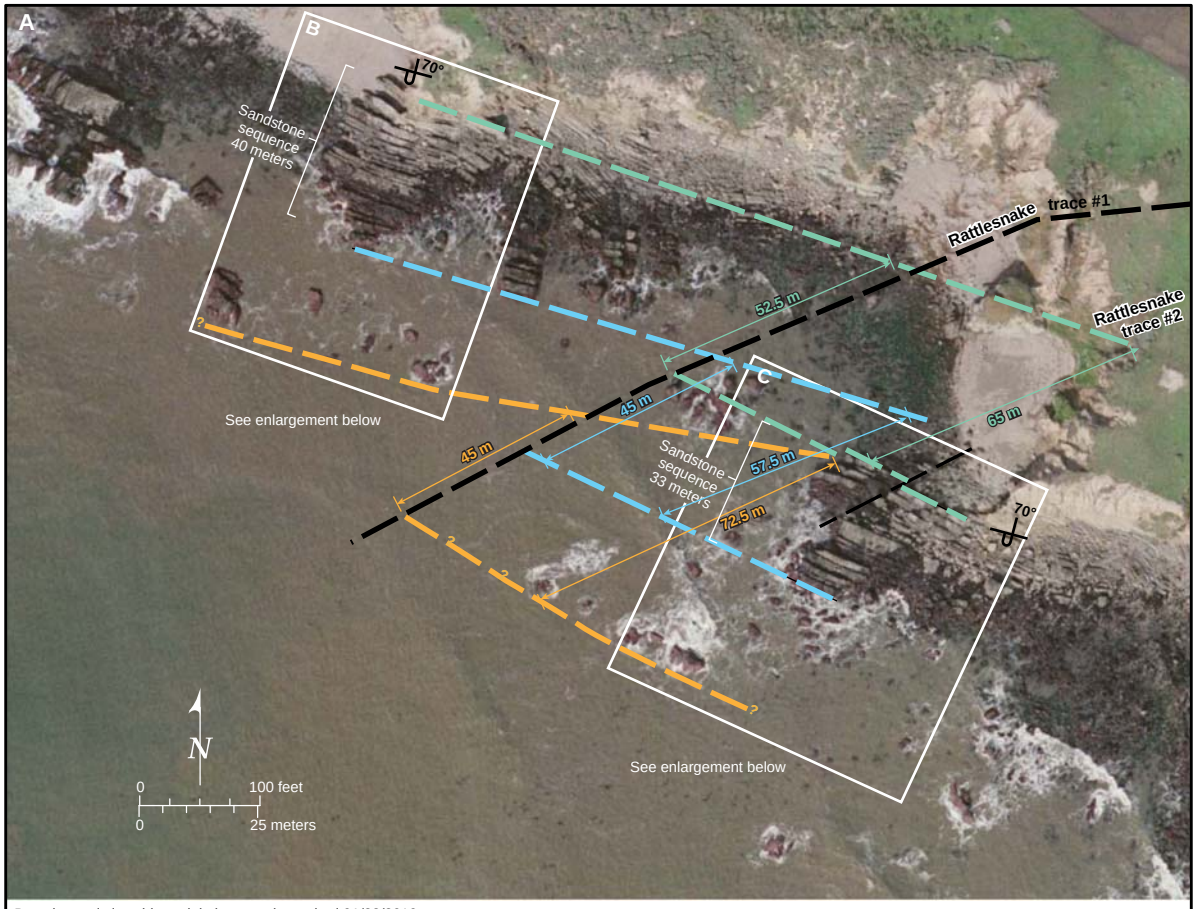

Base image is low tide aerial photograph, aquired 01/28/2010

Interpreted Correlation

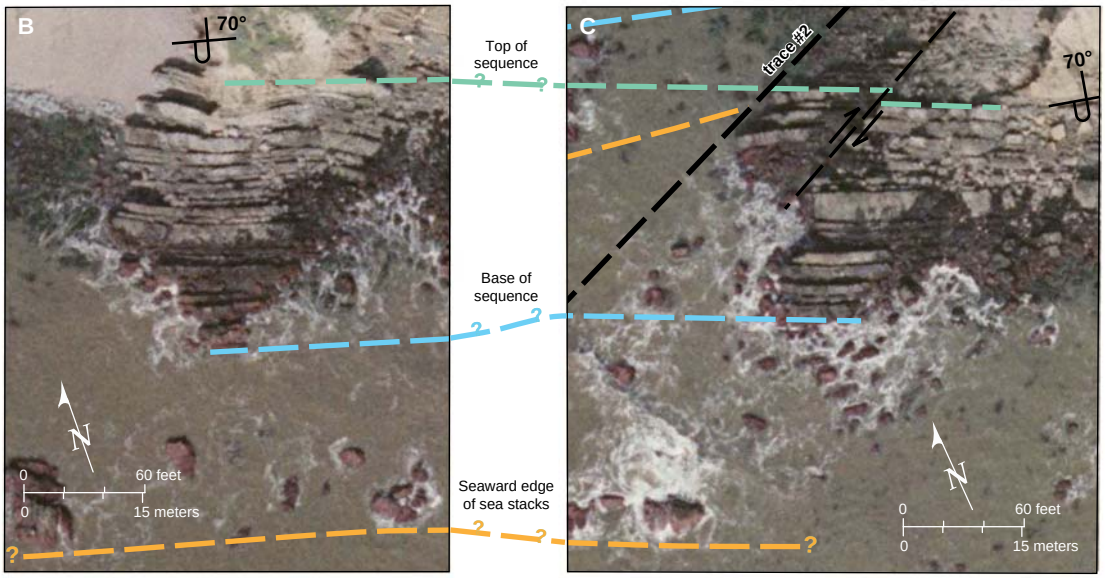

See Figure 4-14 for location

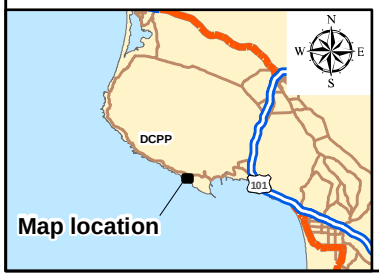

Explanation

- Top of sequence
- Base of sequence
- Seaward edge of sea stacks
- Faults, approximately located
- Strike and dip of overturned bed (70°)

Apparent offset of Cretaceous sandstone beds across the Rattlesnake fault, San Luis Bay fault zone

SHORELINE FAULT ZONE STUDY

Pacific Gas and Electric Company

Figure **4-23**

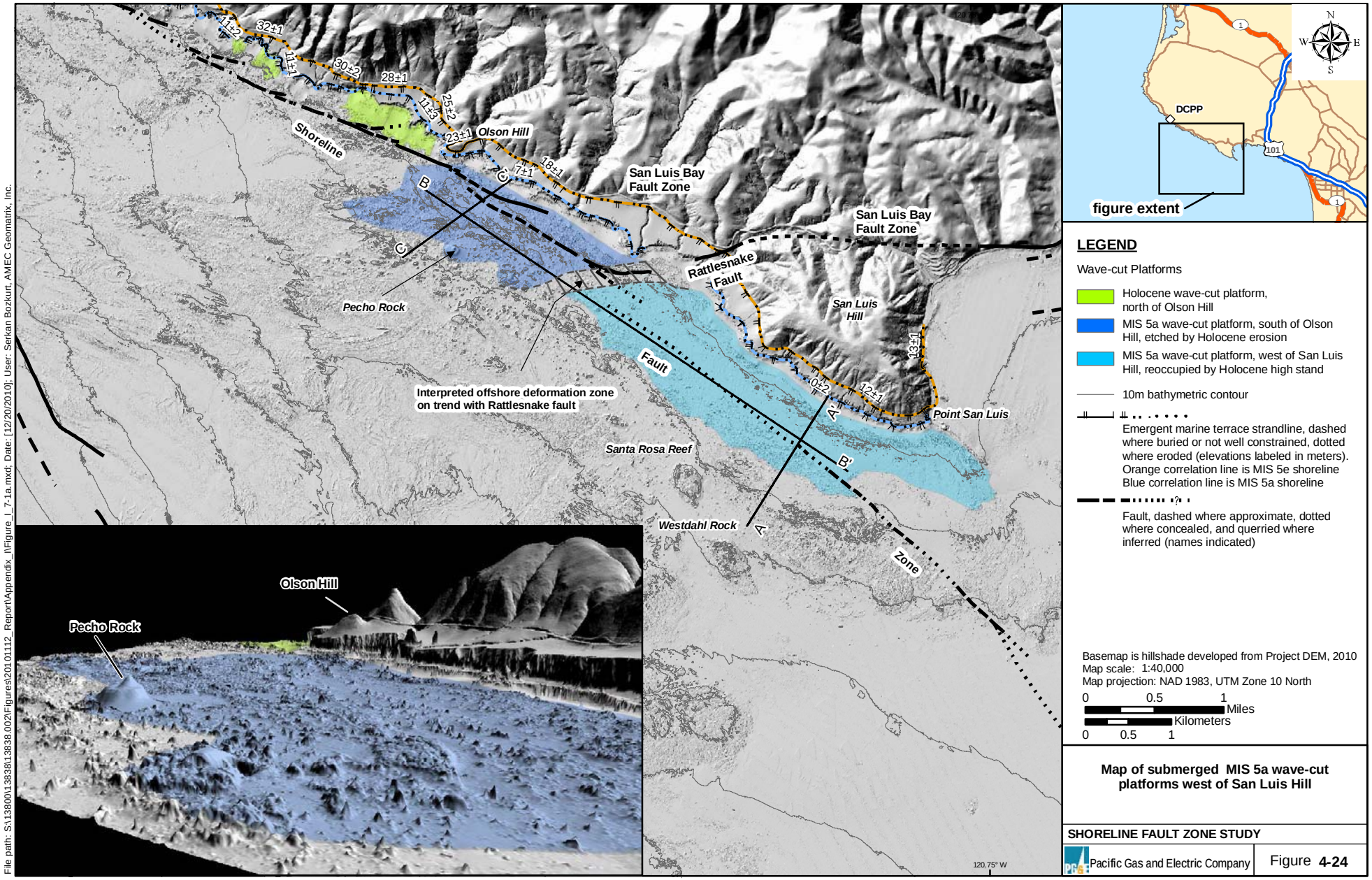
Shoreline
Olson Hill
San Luis Bay Fault Zone
San Luis Bay Fault Zone
Rattlesnake Fault
San Luis Hill
Pecho Rock
Fault
Interpreted offshore deformation zone on trend with Rattlesnake fault
Point San Luis
Santa Rosa Reef
Westdahl Rock
Zone
32±1
1±2
11±1
30±2
28±1
25±2
11±3
23±1
18±1
7±1
13±1
12±1
0±2
A
A'
B
B'
C
C'
120.75° W
Olson Hill
Pecho Rock
DCPP
figure extent
N
S
E
W
101
1
LEGEND
Wave-cut Platforms
Holocene wave-cut platform, north of Olson Hill
MIS 5a wave-cut platform, south of Olson Hill, etched by Holocene erosion
MIS 5a wave-cut platform, west of San Luis Hill, reoccupied by Holocene high stand
10m bathymetric contour
Emergent marine terrace strandline, dashed where buried or not well constrained, dotted where eroded (elevations labeled in meters). Orange correlation line is MIS 5e shoreline Blue correlation line is MIS 5a shoreline
Fault, dashed where approximate, dotted where concealed, and querried where inferred (names indicated)
Basemap is hillshade developed from Project DEM, 2010
Map scale: 1:40,000
Map projection: NAD 1983, UTM Zone 10 North
0 0.5 1 Miles
0 0.5 1 Kilometers
Map of submerged MIS 5a wave-cut platforms west of San Luis Hill
SHORELINE FAULT ZONE STUDY
Pacific Gas and Electric Company
Figure 4-24
File path: S:\138600\13838\13838.002\Figures\20101112_Report\Appendix_I\Figure_I_7-1a.mxd; Date: [12/20/2010]; User: Serkan Bozkurt, AMEC Geomatrix, Inc.

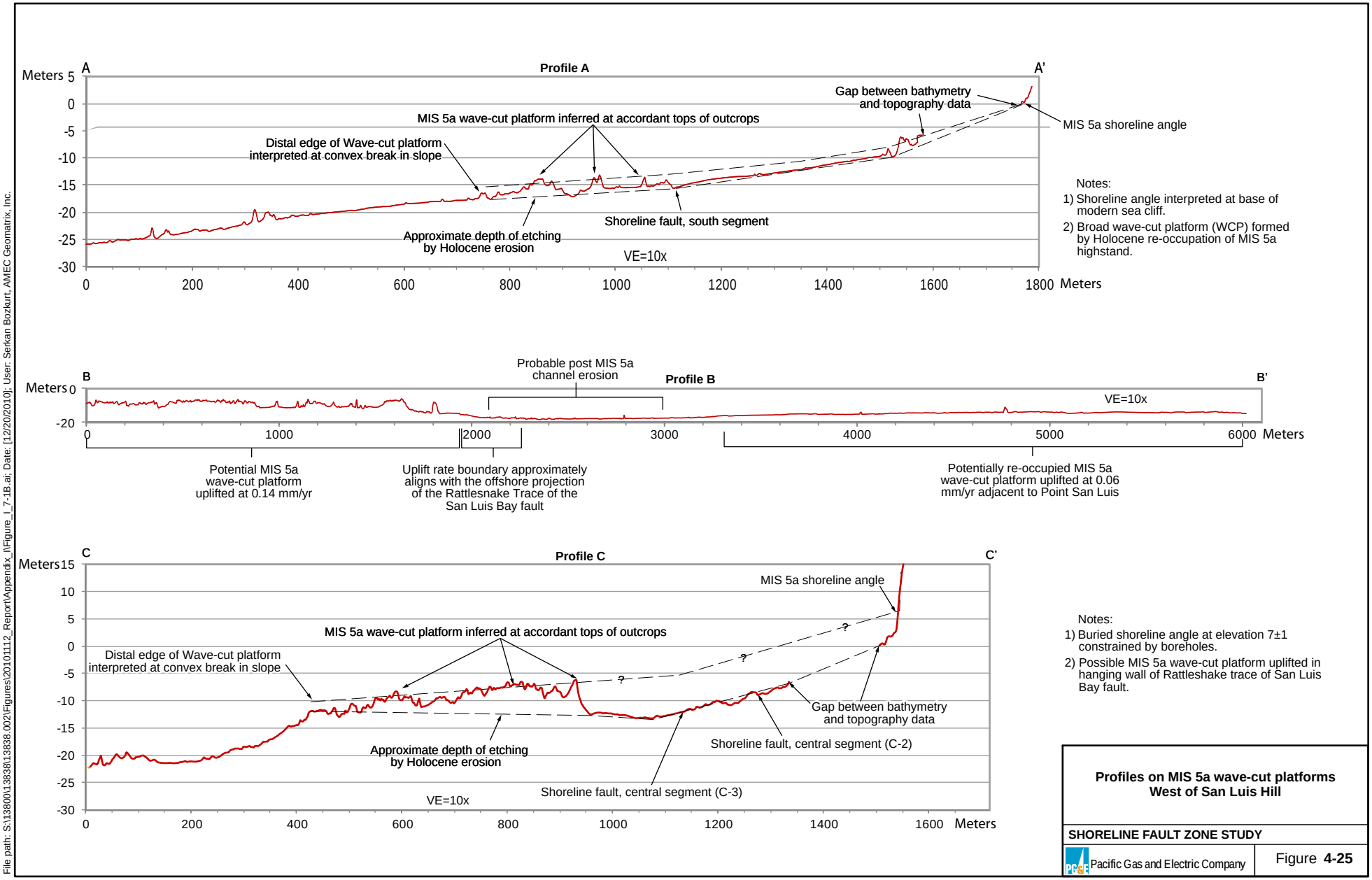
Profile A
A
A'
Meters
Gap between bathymetry and topography data
MIS 5a shoreline angle
MIS 5a wave-cut platform inferred at accordant tops of outcrops
Distal edge of Wave-cut platform interpreted at convex break in slope
Shoreline fault, south segment
Approximate depth of etching by Holocene erosion
VE=10x
Meters
Notes:
1) Shoreline angle interpreted at base of modern sea cliff.
2) Broad wave-cut platform (WCP) formed by Holocene re-occupation of MIS 5a highstand.
Probable post MIS 5a channel erosion
Profile B
B
B'
VE=10x
Meters
Potential MIS 5a wave-cut platform uplifted at 0.14 mm/yr
Uplift rate boundary approximately aligns with the offshore projection of the Rattlesnake Trace of the San Luis Bay fault
Potentially re-occupied MIS 5a wave-cut platform uplifted at 0.06 mm/yr adjacent to Point San Luis
Profile C
C
C'
Meters
MIS 5a shoreline angle
MIS 5a wave-cut platform inferred at accordant tops of outcrops
Distal edge of Wave-cut platform interpreted at convex break in slope
Gap between bathymetry and topography data
Shoreline fault, central segment (C-2)
Approximate depth of etching by Holocene erosion
Shoreline fault, central segment (C-3)
VE=10x
Meters
Notes:
1) Buried shoreline angle at elevation 7±1 constrained by boreholes.
2) Possible MIS 5a wave-cut platform uplifted in hanging wall of Rattleshake trace of San Luis Bay fault.
Profiles on MIS 5a wave-cut platforms West of San Luis Hill
SHORELINE FAULT ZONE STUDY
Pacific Gas and Electric Company
Figure 4-25
File path: S:\13800\13838\13838.002\Figures\20101112_Report\Appendix_I\Figure_I_7-1B.ai; Date: [12/20/2010]; User: Serkan Bozkurt, AMEC Geomatrix, Inc.

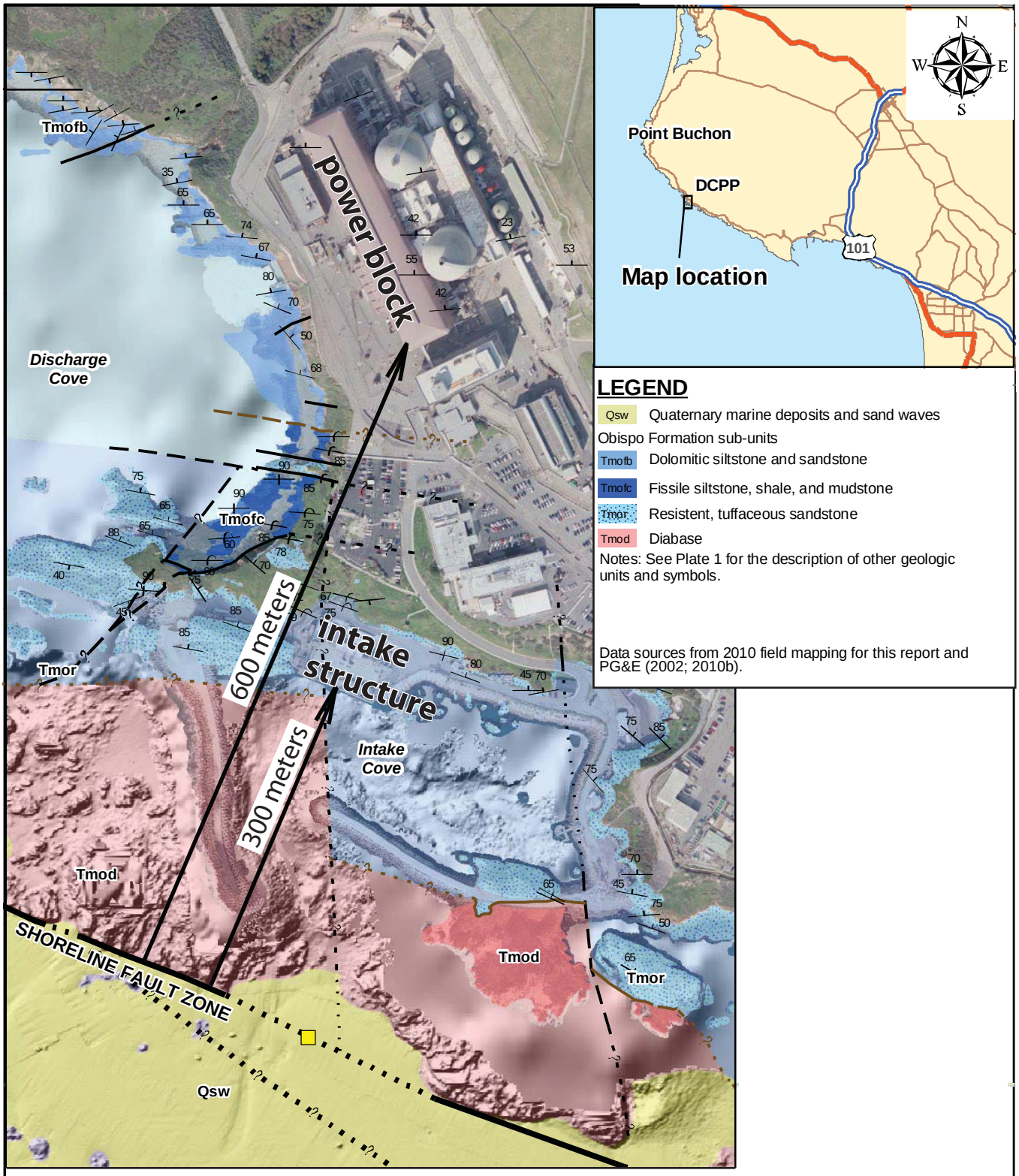

Map projection: NAD 1983, UTM Zone 10 North

0 500 1,000 Feet

0 100 200 Meters

Distance to DCPP power block and Intake structure from Shoreline fault zone

SHORELINE FAULT STUDY

Pacific Gas and Electric Company

Figure **4-26**